

Neurobiology

# Dysregulation of Stathmin, a Microtubule-Destabilizing Protein, and Up-Regulation of Hsp25, Hsp27, and the Antioxidant Peroxiredoxin 6 in a Mouse Model of Familial Amyotrophic Lateral Sclerosis

Christoph W. Strey,\* Daniel Spellman,\*  
Anna Stieber,\* Jacqueline O. Gonatas,\*  
Xiaosong Wang,<sup>†</sup> John D. Lambris,\* and  
Nicholas K. Gonatas\*

From the Department of Pathology and Laboratory Medicine,\*  
University of Pennsylvania Medical Center, Philadelphia,  
Pennsylvania; and the Jackson Laboratory,<sup>†</sup> Bar Harbor, Maine

**Gain-of-function mutations of the Cu/Zn superoxide dismutase (SOD1) gene cause dominantly inherited familial amyotrophic lateral sclerosis. The identification of differentially regulated proteins in spinal cords of paralyzed mice expressing SOD1<sup>G93A</sup> may contribute to understanding mechanisms of toxicity by mutant SOD1. Protein profiling showed dysregulation of Stathmin with a marked decrease of its most acidic and phosphorylated isoform, and up-regulation of heat shock proteins 25 and 27, peroxiredoxin 6, phosphatidylinositol transfer protein- $\alpha$ , apolipoprotein E, and ferritin heavy chain. Stathmin accumulated in the cytoplasm of 30% of spinal cord motor neurons with fragmented Golgi apparatus. Overexpression of Stathmin in HeLa cells was associated with collapse of microtubule networks and Golgi fragmentation. These results, together with the decrease of one Stathmin isoform, suggest a role of the protein in Golgi fragmentation. Mutant SOD1 co-precipitated and co-localized with Hsp25 in neurons and astrocytes. Mutant SOD1 may thus deprive cells of the anti-apoptotic and other protective activities of Hsp25. Astrocytes contained peroxiredoxin 6, a unique nonredundant antioxidant. The up-regulation of peroxiredoxin 6 probably constitutes a defense to oxidative stress induced by SOD1<sup>G93A</sup>. Direct effects of SOD1<sup>G93A</sup> or sequential reactions triggered by the mutant may cause the protein changes. (*Am J Pathol* 2004, 165:1701–1718)**

Amyotrophic lateral sclerosis (ALS) is a world-wide, fatal neurodegenerative disease characterized by loss of motor neurons in the cerebral cortex, brain stem, medulla, and spinal cord and by the proliferation of astrocytes.<sup>1</sup> The annual incidence of sporadic ALS in nonendemic areas is 1.0 per 100,000.<sup>2,3</sup> Among the indigenous population of Guam, ALS occurs frequently in combination with parkinsonism and dementia.<sup>3</sup> The cause(s) of the majority of sporadic ALS cases is unknown.

The discovery of mutations in the gene encoding Cu,Zn superoxide dismutase (SOD1) in certain cases of dominantly inherited familial amyotrophic lateral sclerosis (fALS),<sup>4,5</sup> and the generation of a transgenic mouse model that recapitulated the clinical and neuropathological features of the disease,<sup>6</sup> gave hope for understanding the mechanisms of neuronal death, "Yet, understanding the toxicity of SOD1 mutants has been surprisingly challenging."<sup>7</sup> A variety of hypotheses have been advanced to explain the toxicity of mutant SOD1 in transgenic mice. These include aberrant Cu-mediated catalysis, nitration of tyrosine residues, the generation of toxic hydroxyl radicals, disruption of the neuronal NO synthetase, aggregation of mutant SOD1, mitochondrial dysfunction, triggering of mechanisms for apoptotic death, glutamate excitotoxicity, and adverse effects of cytoplasmic inclusions of neurofilaments or peripherin.<sup>7</sup> To gain further information on any one or more of the above hypotheses, and to identify proteins that may be involved in mutant SOD1 toxicity, we performed protein profiling of pooled spinal cord homogenates from paralyzed mice

Supported by the National Institutes of Health (grant NS 36732) and the Dr. Ralph and Sallie Weaver Professorship of Research Medicine (to N.K.G.).

Accepted for publication July 26, 2004.

Address reprint requests to Nicholas K. Gonatas, University of Pennsylvania Medical Center, 609 Stellar-Chance Labs., 422 Curie Blvd., Philadelphia, PA, 19104-6100. E-mail: gonatasn@mail.med.upenn.edu.

and from 6- to 8-week-old asymptomatic mice that expressed the mutant SOD1<sup>G93A</sup>. Age-matched, symptom-free transgenic mice that expressed the wild-type human SOD1 (WT) and normal littermates that did not express mutant SOD1 were used as controls.

We discovered a so-far unsuspected differential regulation of the most acidic isoform of the microtubule-destabilizing protein Stathmin, heat shock proteins (Hsp) 25 and 27, the anti-oxidant protein peroxiredoxin 6 (PRDX6), as well as of phosphatidylinositol transfer protein (PITP)- $\alpha$ , apolipoprotein E, and ferritin heavy chain. We decided to examine the roles of Stathmin, Hsp25, and PRDX6 in the pathogenesis of the disease.

The emergence of the microtubule-destabilizing protein Stathmin<sup>8-10</sup> as a possible factor in mutant SOD1-mediated toxicity may be significant, because microtubules are essential for the structural integrity of the Golgi apparatus that is fragmented by microtubule-depolymerizing drugs,<sup>11,12</sup> in sporadic ALS, in familial ALS caused by SOD1 mutations, and in transgenic mice expressing an SOD1 mutant, months before the onset of paralysis.<sup>13-15</sup> It should be stressed that mice that expressed the WT human SOD1, in this and in a previous study, were symptom-free and had a normal Golgi apparatus on spinal cord motor neurons as late as 289 days of age.<sup>15</sup>

Fragmentation of the neuronal Golgi apparatus was characterized by others as one of the hallmarks in the transgenic mouse model of ALS.<sup>16</sup> The discovery of differentially regulated Hsp25 and Hsp27 confirms results obtained by others from cultured cells.<sup>17</sup> We confirmed the *in vivo* co-precipitation of SOD1 with Hsp25, a finding consistent with the hypothesis that the binding of mutant SOD1 to Hsp25 deprives cells of the anti-apoptotic and other protective activities of Hsp25.<sup>17</sup> In addition, we found that Hsp25 was localized in reactive astrocytes of paralyzed mice, consistent with the proposed involvement of astrocytes in the pathogenesis of the motor neuropathy induced by mutant SOD1.<sup>18,19</sup>

Oxidative stress has been implicated in the toxicity by mutant SOD1.<sup>7,16</sup> Therefore, the up-regulation of the anti-oxidant PRDX6 may be a defensive reaction by an enzyme that, so far, has not been implicated in functions of the central nervous system. The results obtained by two-dimensional gel profiling were confirmed by Western blotting. Immunocytochemistry was used to localize the enzyme in reactive astrocytes of paralyzed mice, which lends further support to the idea that astrocytes are indeed involved in the pathogenesis of the disease.<sup>18,19</sup>

No significant changes in Stathmin, Hsp25, Hsp27, and PRDX6 were noted in 6- to 8-week-old asymptomatic mice expressing the SOD1<sup>G93A</sup> mutation. Future studies in mice of intermediate ages may establish the temporal sequence of up- or down-regulated proteins and contribute to the identification of early, and perhaps primary, events associated with mutant SOD1 toxicity. Future studies performed in subcellular fractions and in spinal cord motor neurons isolated with a laser microdissector may reveal changes in low-abundance proteins playing a role in the pathogenesis of the disease.

## Materials and Methods

### Antibodies and Reagents

The methods for the generation and specificity of polyclonal antibodies against the *cis*-Golgi matrix protein GM130 and of polyclonal and monoclonal antibodies against the medial Golgi protein MG160 have been published.<sup>20-22</sup> Affinity-purified sheep anti-human SOD1 antibody was from Calbiochem (San Diego, CA). A rabbit anti-SOD1 antibody, raised against rat SOD1, was from Stressgen (Victoria, BC, Canada). A rabbit anti-SOD1, raised against full-length recombinant SOD1, was from Santa Cruz Biotechnology (Santa Cruz, CA). Antisera against SCLIP and SCG10, members of the Stathmin phosphoprotein family, and against the phosphorylated serine 16 of Stathmin, which reacts with all phosphoforms of the protein, were gifts from A. Sobel (INSERM, Paris, France).<sup>10</sup> Antibody against  $\alpha$ -tubulin was purchased from Sigma (St. Louis, MO). The preparation of the antiserum against a unique peptide of PRDX6, FPKGVFT-KELPSGKKYLRYK, was described;<sup>23</sup> the encoded protein is 224 amino acids in length with a predicted size of 25 kd but the protein migrates in polyacrylamide gel electrophoresis gels at ~32 kd (see Figure 11).<sup>23</sup> An antiserum against the C-terminus residues 134 to 149 of rat Stathmin, which detects all isoforms of the protein, was purchased from Calbiochem.<sup>24</sup> A rabbit anti-Hsp antibody was purchased from Stressgen. Monoclonal mouse antibody to glial fibrillary acidic protein (GFAP) was gift from Dr. J.Q. Trojanowski (University of Pennsylvania, Philadelphia, PA). DAPI (4'-6-diaminidine-2'-phenylindone diHCL) was from Sigma (St. Louis, MO).<sup>25</sup>

### Selection of Transgenic Mice Carrying the G93A Mutation

Founder mice, heterozygous for the G93A mutation of the human gene for SOD1, were purchased from the Jackson Laboratories (Bar Harbor, ME). These mice were made available to the Jackson Laboratories by M.E. Gurney (de CODE Genetics, Reykjavik, Iceland) who developed the first transgenic animal model of fALS.<sup>6</sup> B6SJL/J+/+ females were paired with B6SJL-Tgn(SOD1-G93A)2GUR hemizygous male carriers; 50% of the progeny from these pairs are carriers of the G93A transgene. The littermates that did not express mutant SOD1 were used as age-matched controls. Another cohort of control mice, expressing the WT human SOD1 [B6SJL-Tgn(SOD1)2GUR], were also purchased from the Jackson Laboratories and were maintained until they reached suitable ages. Carrier selection was accomplished by polymerase chain reaction genotyping with DNA extracted from a 0.5-cm-long segment of mouse tail, using primers that amplify a 236-bp product from exon 4 of the human SOD1 gene within the transgene construct, or a 324-bp product of the endogenous mouse interleukin (IL)-2 gene (control), as described.<sup>26</sup>

### *Western Blotting and Immunoprecipitations*

Western blotting was performed with standard methods as described.<sup>20,27</sup> For immunoprecipitations, spinal cords from paralyzed mice expressing SOD1<sup>G93A</sup>, or from age-matched controls that expressed the wild-type human SOD1 (WT), were homogenized at 4°C in a buffer containing 1% Triton X-100, 20 mmol/L Tris-HCl, pH 7.5, 0.15 mol/L NaCl, and a cocktail of protease inhibitors. Mice were euthanized with CO<sub>2</sub>, the spinal cords were immediately removed, plunged in liquid nitrogen, and stored at -80°C until use. Extracts were cleared by centrifugation at 20,000 × *g* and 135 μg of protein from the supernatants were rotated overnight at 4°C with a monoclonal anti-SOD1 antibody (SZ147, Sigma), an antibody against Hsp25 (Stressgen), or with an irrelevant monoclonal antibody against the MG160 protein.<sup>20</sup> The immunoprecipitate was precipitated by 30 μl of a mixture of Protein A/G-Sepharose (Amersham Biosciences, Piscataway, NJ) by incubation for 4 hours at 4°C. The beads were washed extensively with 0.1% Triton X-100, 10 mmol/L Tris-HCl, pH 7.5, 0.15 mol/L NaCl, boiled in Laemmli sample buffer, and centrifuged; the supernatant was applied to a 14% sodium dodecyl sulfate acrylamide gel. After electrophoresis, the transferred proteins from immunoprecipitations with anti-SOD1 antibody were probed with an antibody against Hsp25, and proteins from immunoprecipitations with an anti-Hsp25 antibody or an irrelevant antibody, were probed with an anti-SOD1 antibody. All blots were developed by the chemiluminescent reaction.

### *Plasmid Preparation and Transfections*

The cDNA of human Stathmin was a gift from Dr. Donna George (University of Pennsylvania, Philadelphia, PA).<sup>28</sup> The cDNA was introduced into the pBK-CMV vector from Stratagene as previously described.<sup>29</sup> This was used to transfect CHO or HeLa cells with Lipofectamine-plus (Gibco-BRL, Division of Invitrogen, Gaithersburg, MD) as previously described.<sup>29</sup>

### *Immunohistochemistry and Fluorescence*

#### *Labeling*

The methods of tissue fixation, permeabilization, and immunolabeling were described previously.<sup>26</sup> In brief, mice were euthanized in dry ice and perfused via the left ventricle with 1% paraformaldehyde in 0.1 mol/L phosphate buffer, pH 7.35. Ten-μm-thick frozen sections of the spinal cord were cut, permeabilized with 0.5% Triton X-100, and nonspecific antibody binding sites were blocked with 2% fish gelatin in 0.5% Triton X-100 in buffered physiological saline.<sup>26</sup> For double immunostaining of tubulin and Stathmin, cultured cells were fixed for 6 minutes in 100% methanol at -20°C. All other cells were fixed in 1% paraformaldehyde for 20 minutes at room temperature. For single immunostaining, sections of mouse spinal cord were incubated overnight in the primary antibody followed by biotinylated goat anti-rabbit

IgG and ABC Elite (Vector Laboratories, Burlingame, CA). For double immunostaining of Hsp25 and GFAP, sections were incubated in combined primary antibodies, then in biotinylated donkey anti-rabbit IgG (Jackson ImmunoResearch, West Grove, Pa) mixed with goat anti-mouse IgG (ICN, Irvine, CA), followed by rhodamine-labeled donkey anti-sheep IgG (Jackson ImmunoResearch) mixed with avidin coupled with fluorescein isothiocyanate (Vector Laboratories). For double immunostaining of Hsp25 and SOD1, sections were incubated in combined primary antibodies, then in biotinylated donkey anti-sheep IgG mixed with rhodamine-labeled donkey anti-rabbit IgG (Jackson ImmunoResearch), followed by avidin coupled with fluorescein isothiocyanate. For the other double immunostains, sections or HeLa cells were incubated in the combined primary antibodies, then in biotinylated horse anti-mouse IgG (Vector Laboratories) mixed with rhodamine-labeled donkey anti-rabbit IgG, followed by avidin coupled with fluorescein isothiocyanate.

### *Protein Profiling: Two-Dimensional Gel Electrophoresis and Mass Spectrometry*

Pooled spinal cords from five control mice (age-matched normal littermates that did not express the mutant, or mice that overexpressed the WT human SOD1) and five SOD1<sup>G93A</sup> paralyzed mice were used for two-dimensional gel electrophoresis. A second set of mouse spinal cords consisted of five pooled spinal cords from 6- to 8-week-old asymptomatic mice expressing SOD1<sup>G93A</sup> and five spinal cords from 6- to 8-week-old mice expressing the WT human SOD1. Spinal cords, frozen at -80°C, were homogenized with mortar and pestle on liquid nitrogen. The tissue powder was resuspended in lysis buffer consisting of 40 mmol/L Tris, 7 mol/L urea, 2 mol/L thiourea, 4% Chaps, 10 mmol/L 1,4-dithioerythritol, 1 mmol/L ethylenediaminetetraacetic acid, and protease inhibitors. The suspension was homogenized by sonication for 30 seconds and centrifuged at 150,000 × *g* for 60 minutes. The protein content was determined by the Coomassie blue method.<sup>30</sup> Two-dimensional gel electrophoresis was performed for each sample pool at least in triplicates as reported.<sup>31</sup> For the first dimension, 400 μg of protein were applied on 11-cm immobilized pH 5 to 8 linear gradient strips with ampholytes (pI: 3.5 to 10) (Bio-Rad, Hercules, CA). Isoelectric focusing started at 200 V and the voltage was gradually increased to 8000 V and kept constant until 70,000 volt-hours were reached. Separation for the second dimension was performed on 12.5% Tris/HCl gels (Bio-Rad). The gels were run at 40 mA per gel, in a Criterion gel apparatus (Bio-Rad). After protein fixation for 12 hours in 40% methanol, containing 5% acetic acid, the gels were stained with Coomassie Blue (Pierce Biotechnology, Rockford, IL) for 24 hours. After destaining with water for 12 hours, the gels were scanned in a densitometer (Amersham Biosciences). The resulting digital images were analyzed and quantified using the ImageMaster 2D Elite software (Amersham Biosciences). For comparisons of abundance among gels, normalization was done against the total intensity of all spots

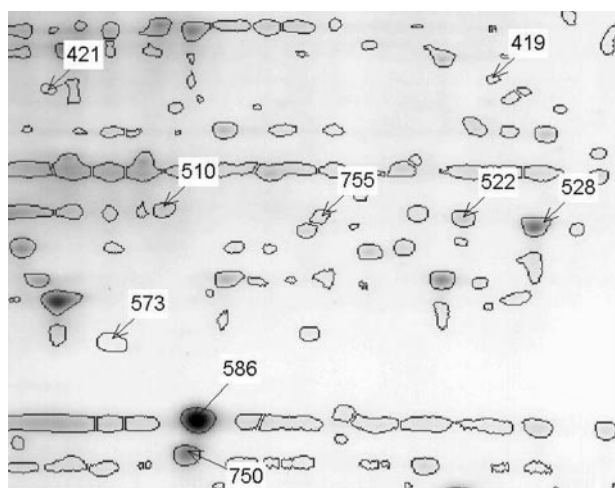


**Figure 1.** Two-dimensional gel map of pooled spinal cord extracts from five WT animals containing the spots with significant abundance changes. Areas containing the Stathmin spot and the Hsp25 spot are compared in greater detail in Figure 2 (under A for Stathmin and B for Hsp25). The location of the spots with significant and greater than twofold abundance differences between the mutant and WT samples are labeled with their corresponding identification numbers. Note: in this and in the subsequent legends, WT is for mice that express the wild-type human SOD1.

present in the gel. The relative spot intensities were then subjected to statistical analysis by applying the nonparametric test of Mann and Whitney. *P* values less than 0.5 were considered statistically significant.

For mass spectrometry, the spots of interest were excised from the gels and sequentially washed for 1 hour in 50 mmol/L  $\text{NH}_4\text{HCO}_3$  and in 50% acetonitrile before gel digestion. After washing, gel pieces were shrunken in acetonitrile, dried, and then rehydrated with 50 mmol/L  $\text{NH}_4\text{HCO}_3$  containing 0.01% of sequence grade trypsin (Promega, Madison, WI). After overnight digestion at room temperature, the peptides were extracted twice with 50% acetonitrile and 0.1% trifluoroacetic acid applying one sequence of vortexing and sonication (each for 20 minutes). After drying, the peptide mixtures were resuspended in 5  $\mu\text{l}$  of 0.1% TFA, 1:1, mixed with  $\alpha$ -cyano-4-hydroxycinnamic acid matrix (10 mg/ml in 30% acetonitrile/0.1% TFA, v/v) and spotted on a MALDI plate. Mass spectrometry analysis was performed with a VG 2E Tofspec laser desorption time of flight mass spectrometer (Waters, Milford, MA).

## Results

### *Changes of Protein Abundance in the Spinal Cords of Paralyzed Mice Expressing SOD1<sup>G93A</sup> (Figure 1, Figure 2, Table 1)*

Using two-dimensional gel electrophoresis, the proteome of spinal cords from 6- to 8-week-old (asymptomatic) and 24- to 28-week-old mice (paralyzed), both expressing SOD1<sup>G93A</sup>, were compared to the proteome of age-matched expressers of wild-type human SOD1, or age-matched asymptomatic littermates; two-dimensional gel electrophoresis allows for the quantitative comparison of a large number of proteins simultaneously and is there-

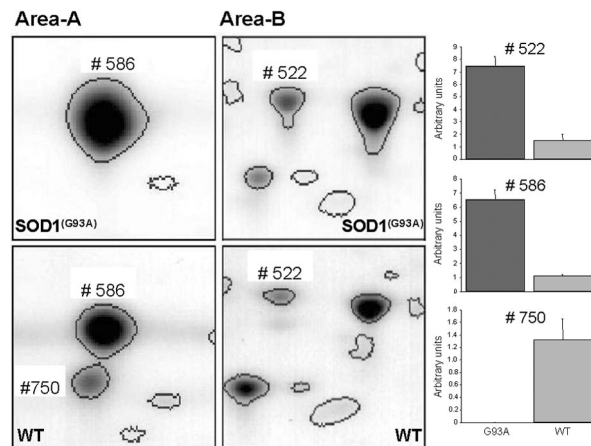


**Figure 2.** Comparison of magnified gel areas (as highlighted in Figure 1) and spot abundance changes from WT and SOD1<sup>G93A</sup> mice. The **left** panel displays the gel areas of spot 586 (SOD1<sup>G93A</sup>) and spot 750 (Stathmin) (area A), and spot 522 (Hsp25) (area B) (compare also Figure 1) from a representative gel with protein extracts from five pooled spinal cords from SOD1<sup>G93A</sup> mice (**top**) and their controls (**bottom**). The bar plots on the **right** display the abundance differences of the corresponding spots. Hsp25 (spot 522) and SOD1<sup>G93A</sup> (spot 586) are more abundant in the SOD1<sup>G93A</sup> mice, whereas Stathmin (spot 750) is only present in the WT mice. Spot 586 in the WT samples, which is located in the same area as the SOD1<sup>G93A</sup> protein in the corresponding gels run with protein extracts from mutant mice, could not be identified using mass spectrometry, and is classified as unknown.

fore able to reveal possible differences in protein abundance between SOD1<sup>G93A</sup> mice and their controls.

To optimize protein separation, and at the same time analyze a large proportion of the tissue proteome in one step, a pI range of 5 to 8 was chosen for the first dimension. Preliminary experiments with broad range (pI range, 3 to 10) immobilized pH gradient strips revealed that ~70 to 80% of the protein spots were present between a pI range of 5 to 8 (data not shown).

Proteome analysis by two-dimensional gel electrophoresis of spinal cords from paralyzed SOD1<sup>G93A</sup>-expressing mice revealed nine spots that differed more than twofold in abundance when compared to control (*P* < 0.05, Table 1). This represented ~1.3 to 1.5% of the more than 600 spots identified. All detected and quantified spots were compared on the basis of their relative abundance in relation to the total abundance of all spots detected in the corresponding gel. This normalization allows the comparison of spots between gels independent of loading and staining intensity differences between individual gels. Low-abundance proteins may have been missed. The range of differences on the basis of standard errors is presented in Table 1. Out of this group of spots eight distinct proteins were identified by mass spectrometry (Table 1). Spot 586 was identified as the SOD1 protein, which by Western blot analysis of the two-dimensional gel reacted with an antibody against human SOD1 (data not shown). Spot 419 was identified as PITP- $\alpha$ , which has been implicated in functions of the endoplasmic reticulum functions involving lipid metabolism and transport. Mice lacking PITP- $\alpha$  showed spinocerebellar degeneration and other abnormalities.<sup>32</sup>

Spot 421 was apolipoprotein E (apoE) (Figure 1). The involvement of apoE in the pathogenesis of the disease in mice expressing SOD1<sup>G93A</sup> has been reported.<sup>33</sup> Spots

**Table 1.** Altered Levels of Proteins in SOD1<sup>G93A</sup> Mice (Paralyzed) Versus Wild-Type Mice

Spot number	Two-dimensional gel coordinates: pI/MW (kd)	Fold difference compared to wild type ( $P < 0.05$ )	Regulation of protein expression in SOD1 <sup>G93A</sup> mice	Identification (accession number, NCBI)
419	6.8/36	7.9 (4.1–23.1)	Up	Phosphatidylinositol transfer protein alpha (1KCMS)
421	5.6/35	24.8 (13.5–69.5)	Up	Apolipoprotein E (NP_033826)
510	6.1/23	24.8 (13.5–69.5)	Up	Heat shock 27 kDa protein (P14602)
522	7.0/23	4.9 (3.7–6.8)	Up	Heat shock protein 25 kDa (XP_109446)
528	6.0/23	4.5 (3.4–6.1)	Up	Peroxiredoxin 6 (NP_031479)
573	5.8/18	4.2 (2.3–15.3)	Up	Ferritin heavy chain (NP_034369)
586	6.3/14	5.9 (5.3–6.6)	Up	Superoxide dismutase mutant (1FUNA)
750	6.2/12	<100	Down	Stathmin (BAB61894)
755	6.7/23	3.9 (3.3–4.7)	Up	Peroxiredoxin 6 (NP_031479)

Proteins from mouse spinal cords were separated by two-dimensional electrophoresis and identified by MS as described in Material and Methods. Protein spots were quantified from Coomassie blue-stained gels and ImageMaster 2D Elite software. The described protein identities were obtained with Z scores of 1.645 or greater indicating a confidence level of at least the 95th percentile. Column 1 lists the identifying spot numbers; column 2 lists the two-dimensional gel coordinates; column 3 describes how many fold the corresponding spots in the samples from the SOD1<sup>G93A</sup> mice are different from their wild-type controls (range calculated from the standard errors of the spot intensities); column 4 indicates the direction of concentration change in the SOD1<sup>G93A</sup> mice; column 5 contains the protein identities retrieved from the MS analysis with their accession numbers in the NCBI database.

528 and 755 (Figure 1), were identified as PRDX6, which is a widely expressed and a potent protector of oxidative stress.<sup>34</sup> Most likely the two PRDX6 spots represent isoforms that cannot be defined or differentiated by sequencing; spot 573 was identified as ferritin heavy chain (Figure 1). Ferritin serves as an iron storage protein in neuronal and other tissues. Growing evidence suggests that iron homeostasis plays a role in neurodegenerative diseases.<sup>35,36</sup>

The chaperone proteins heat shock protein 27 kd (Hsp27) and 25 kd (Hsp25) were found in spots 510 and 522, respectively (Table 1, Figure 1). Hsp27 and Hsp25 belong to a group of proteins that are involved in protein stabilization and cellular protection. Their functions have already been highlighted in the context of neuronal protection<sup>37</sup> and in the development of various neurodegenerative diseases.<sup>38</sup>

Spot 750, which was only detectable in extracts from control animals (Figures 1 and 2), was identified as Stathmin. The change of abundance of one Stathmin isoform was further confirmed by Western blots in two-dimensional gels using a monoclonal antibody against mouse Stathmin (Figure 3c, asterisk). Stathmin belongs to a group of microtubule-destabilizing proteins that affect the integrity of microtubules and play important roles during mitosis as well as in developmental and postdevelopmental regulatory functions.<sup>8–10</sup>

These described changes of proteins in paralyzed mice might be related to pathogenesis. To rule out the possibility that these proteome alterations were nonspecific epi-phenomena because of the presence of SOD1<sup>G93A</sup>, we performed a similar two-dimensional study in asymptomatic 6- to 8-week-old mice expressing SOD1<sup>G93A</sup> and compared the results to those from age-matched expressors of the WT human SOD1. The younger asymptomatic SOD1<sup>G93A</sup> mice did not show the protein abundance changes, which were described in the older paralyzed mice (data not shown). Changes with significance below the twofold abundance cutoff point could not be detected. Furthermore, we performed two controls for the paralyzed mice, namely an analysis of homogenates of pooled cords from age-matched normal

littermates, and from age-matched mice expressing the wild-type human SOD1 (WT). Apart from the spot of the overexpressed WT human SOD1, no other differences were detected in the spots described above and listed in Table 1 (data not shown).

In summary, the analysis of the spinal cord proteome in paralyzed SOD1<sup>G93A</sup> mice showed down-regulation of one isoform of Stathmin (posttranslational dysregulation?) and up-regulation of, Hsp25, Hsp27, P1TP- $\alpha$ , apoE, PRDX6, and ferritin. These changes were not observed in normal littermates, in mice expressing the WT human SOD1, or in asymptomatic 6- to 8-week-old SOD1<sup>G93A</sup> mice, suggesting that the identified proteins are involved in the later stages of the disease. Alternatively, the methods for protein detection might not be sensitive enough for the detection of similar protein abundance changes in younger animals. It is also possible and probable that changes of proteins that are enriched in certain subcellular fractions are diluted in the homogenates of the entire spinal cord and hence escape detection.

Mass spectroscopic identifications were confirmed by Western blots for Stathmin, Hsp25, and PRDX6 (Figure 3, a to c, and Figure 11) and their significance was further examined by immunocytochemical staining of spinal cord sections or transfected HeLa cells using appropriate antibodies (Figures 4 to 9 and Figure 12). The reported associations of Stathmin, Hsp25, and PRDX6 with important cellular functions<sup>8–10,34,37,38</sup> suggest that these proteins are factors in the pathogenesis of SOD1<sup>G93A</sup> toxicity.

### *Stathmin and Hsp25 Expression Confirmed by Western Blots (Figure 3, a to c)*

Western blots of aliquots from the same extracts of pooled spinal cord homogenates used for protein profiling showed an increase of Hsp25 (Figure 3a), and no significant change of Stathmin (Figure 3b) in comparison to mice expressing the WT human SOD1. The Hsp25

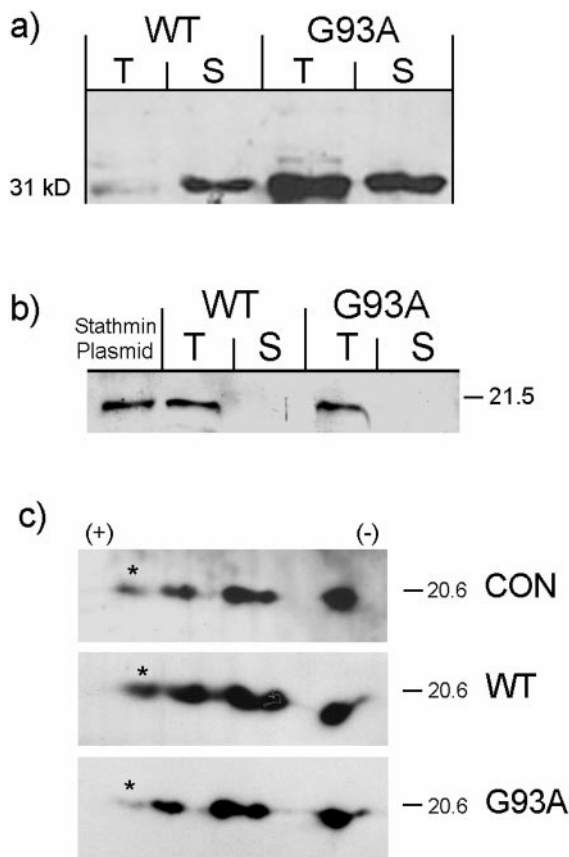


**Figure 3. a:** Hsp25 is up-regulated in pooled extracts from five spinal cords from paralyzed transgenic mice expressing SOD1<sup>G93A</sup>. Immunoblot of spinal cord extracts from age-matched mice expressing the WT and paralyzed transgenic mice expressing SOD1<sup>G93A</sup> probed with anti-Hsp25 antibody. The pellet obtained after centrifugation of the Triton X-100 extract was homogenized in 1% sodium dodecyl sulfate and clarified. Shown are the supernatants from the Triton (T) and sodium dodecyl sulfate (S) extracts. Fifteen  $\mu$ g of protein were loaded in each lane and transferred to nitrocellulose. **b:** WT, extract from five spinal cords of age-matched mice expressing human SOD1; G93A, extract from five spinal cords of paralyzed mice expressing SOD1<sup>G93A</sup>. Unlike Hsp25, Stathmin is found only in the Triton X-100 soluble fraction. Stathmin plasmid: extract of CHO cells transfected with an expression vector for Stathmin (in Materials and Methods) and used in experiments in Figures 6 and 7. **c:** Two-dimensional immunoblot of pooled spinal cord extracts using an antibody against Stathmin; CON, normal age-matched littermates not expressing mutant SOD1; WT, age-matched mice expressing the WT human SOD1; G93A, mice expressing the mutant. **Asterisk** marks the isoform that is down-regulated in the mutant.

protein was found in both a Triton X-100-soluble fraction (T) and in a detergent-insoluble fraction (S) (Figure 3a), whereas Stathmin was found only in the soluble Triton X-100 fraction (T) (Figure 3b).

Western blots of two-dimensional gels showed a selective down-regulation of the most acidic isoform of Stathmin that probably corresponds to its most phosphorylated form (Figure 3c, asterisk; Dr. Sobel, personal communication).<sup>10</sup> Densitometric scanning revealed that this isoform represented only 1.36% of the total in the G93A mutant, in contrast to 6.97% in the normal and 6.43% in the WT control (complete results not shown). Therefore, it is not surprising that on one-dimensional gel electrophoresis and immunoblotting for Stathmin, there was no difference between the WT and the mutant (Figure 3b). Western blots of two-dimensional gels, probed

with an antiserum directed against phosphorylated serine 16, which recognizes all phosphoforms of Stathmin, did not reveal any additional significant differences between the WT and the mutant (not shown).<sup>10</sup>

### *Stathmin, SCG10, and SCLIP Accumulate in Spinal Cord Motor Neurons and Processes of Paralyzed Mice (Figure 4)*

Immunocytochemistry done on sections of control spinal cords did not reveal any staining for Stathmin, except for a rare perinuclear localization, consistent with the Golgi apparatus. This confirms reports on the subcellular distribution of the neuron-enriched soluble Stathmin.<sup>8</sup> In contrast, Stathmin accumulated in the cytoplasm of 30% neurons with fragmented Golgi apparatus, and in processes of paralyzed mice. In control mice, SCG10 and SCLIP, which are membrane-bound phosphoproteins of the Stathmin family, were regularly immunolocalized around nuclei of motor neurons in a pattern suggestive of the Golgi apparatus, as previously reported.<sup>9</sup> In contrast, in paralyzed mice both SCG10 and SCLIP accumulated within the cytoplasm and processes, probably neurites, of spinal cord motor neurons in a pattern identical to that of Stathmin (Figure 4). Immunocytochemistry performed with antisera against the sites 16, 25, and 38 of the Stathmin-phosphorylated forms (donated by A. Sobel<sup>10</sup>) showed fewer neuronal perikarya and processes stained in comparison to results obtained with an antiserum against the C-terminus of Stathmin (not shown). This result raises the possibility of Stathmin dephosphorylation in these cells. Quantitative studies are required to establish the phosphorylation state of Stathmin in these mice.

### *Fragmentation of the Golgi Apparatus in Neurons with Stathmin Accumulation (Figure 5)*

Sections of spinal cords from paralyzed mice were doubly immunostained with antibodies against the Golgi matrix protein GM130, and Stathmin. All motor neurons that contained cytoplasmic accumulations of Stathmin had fragmented or barely detectable Golgi apparatus (Figure 5).

#### *Quantitation*

Sections of spinal cords from seven paralyzed mice were double labeled with an antibody against GM130, a marker of the Golgi apparatus,<sup>22</sup> and Stathmin. A total of 351 neurons in the ventrolateral segments of the anterior (ventral) horns were counted.

#### *Normal Golgi Apparatus*

Normal Golgi apparatus was in the form of a network of perinuclear linear profiles that were immunostained with the antibody.

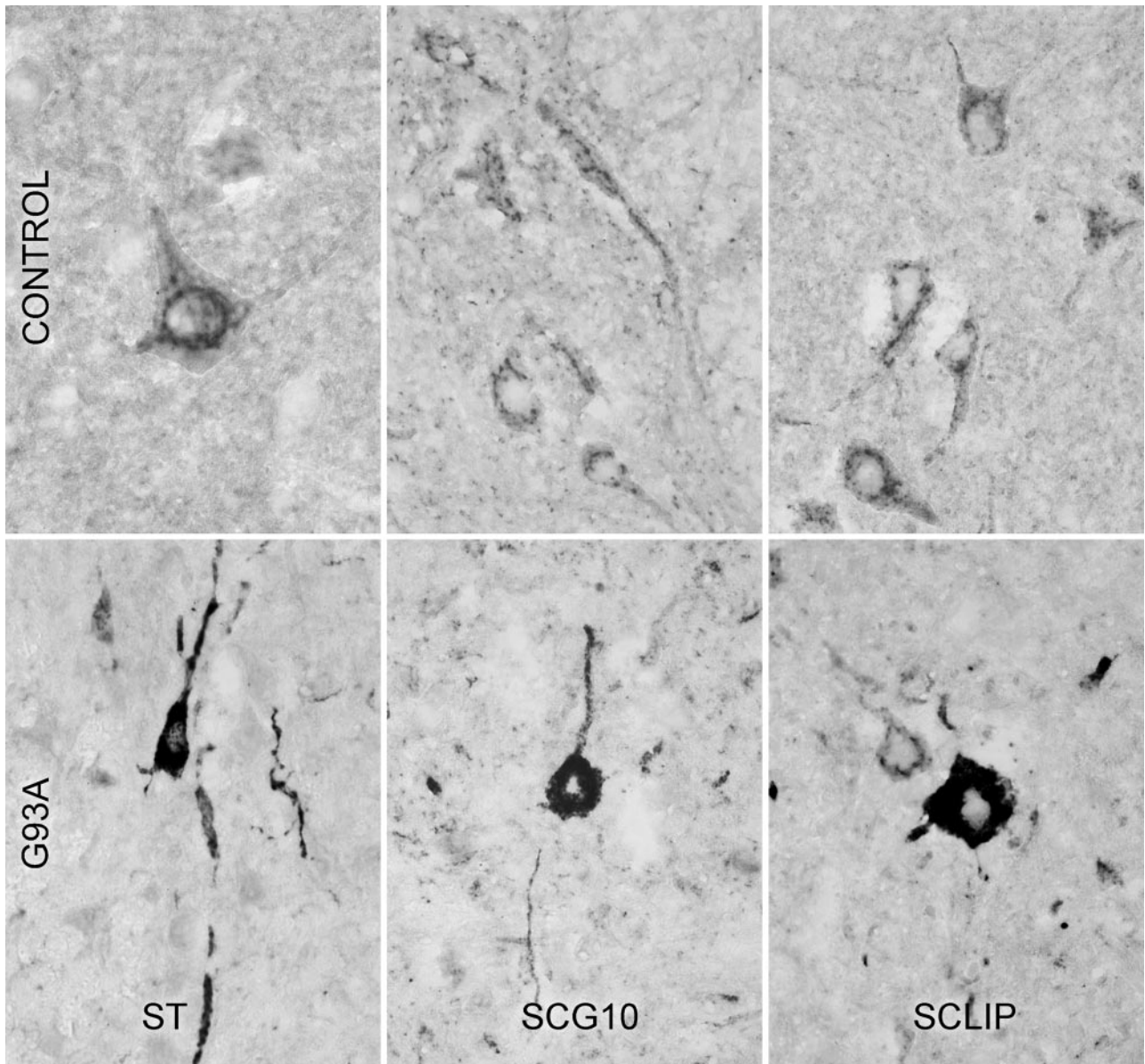


**Figure 4.** Sections of spinal cord from symptom-free mice transgenic for WT human SOD1 (control, **top row**) or paralyzed mice expressing the mutant (G93A, **bottom row**). Immunostained for Stathmin, SCG10, or SCLIP. Note accumulation of Stathmin, SCG10, and SCLIP in neuronal perikarya and processes. Original magnifications,  $\times 400$ .

#### *Fragmented Golgi Apparatus*

Motor neurons containing Golgi profiles in the form of numerous small isolated granules were scored as neurons with fragmented Golgi apparatus. Neurons with remnants of linear *cis*-ternae or a mixture of granular profiles and remnants of *cis*-ternae were counted as normal, although they probably represented neurons with ongoing damage to the Golgi apparatus. Twenty-seven percent of neurons had completely fragmented Golgi apparatus; 30% of these expressed Stathmin. All neurons that expressed Stathmin had fragmented or barely visible Golgi apparatus. Comparison of young, asymptomatic, and paralyzed mice (Table 2) showed that Golgi fragmentation appears before the accumulation of large amounts of Stathmin, which was found mostly in processes. Few

neuronal perikarya remained in paralyzed mice. This accounts for the low score of the Golgi apparatus that was identified and scored only in the perikarya. These results suggest that the initial event(s) causing Golgi fragmentation are Stathmin-independent. Alternatively, the soluble Stathmin may have been lost after weak fixation with 1% paraformaldehyde and extensive washes in detergent (see Materials and Methods).<sup>26</sup> In contrast, the membrane-bound protein marker of the Golgi apparatus MG160, diffuses less and is probably better preserved *in situ* and identified by immunocytochemistry. Furthermore, the bulk of the MG160 protein is within the lumen of the Golgi *cis*-ternae, and that fact may further impede its diffusion.<sup>29</sup> Also, differences in the affinities of antibodies to their respective antigens may explain the earlier detection of Golgi fragmentation.

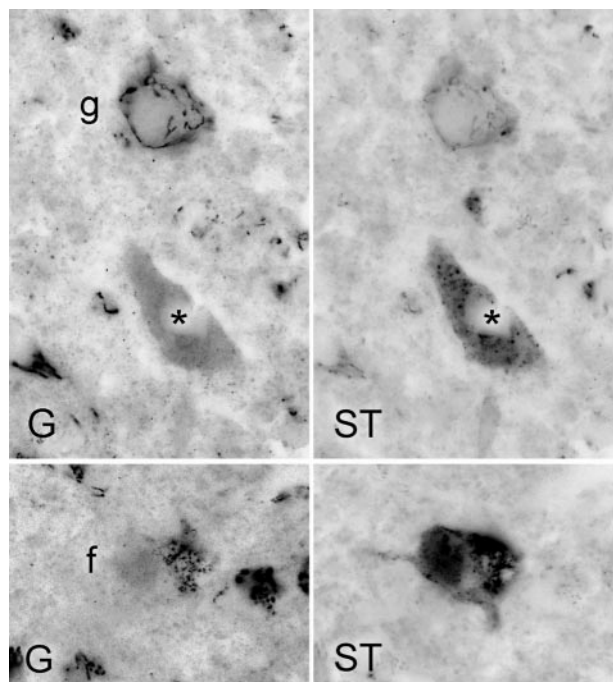


**Figure 5.** Sections of spinal cord from paralyzed mice transgenic for the mutant G93A, double immunostained for Golgi apparatus (G) and Stathmin (ST). In the **top** pair, the cell without Stathmin has a normal Golgi network (g), whereas the cell with accumulated Stathmin has lost all Golgi staining (**asterisk**). The **bottom** pair shows a cell with fragmented Golgi (f) and accumulated Stathmin. Original magnifications,  $\times 600$ .

### Fragmentation of the Golgi Apparatus in HeLa Cells Overexpressing Stathmin (Figure 6)

To further explore a possible relation between the accumulation of cytoplasmic Stathmin and Golgi fragmentation, HeLa cells were transiently transfected with an expression vector for Stathmin (Figure 3b, plasmid).<sup>28</sup> Cells that overexpressed cytoplasmic Stathmin, as judged by an intense immunofluorescence after immunolabeling with an anti-Stathmin antibody, had fragmented Golgi apparatus. Weaker expressors of Stathmin had mostly normal Golgi apparatus. Untransfected cells had a normal Golgi apparatus. It is noteworthy that the nuclei of cells with fragmented Golgi apparatus were not apoptotic as revealed by a DAPI

**Table 2.** Quantitation of Neuronal Golgi Fragmentation (GOLGI) and Stathmin Accumulation (STATH)

	STATH	$\pm$ SEM	GOLGI	$\pm$ SEM
60 to 90 days	0.7	0.33	2.2	0.17
End stage	2.8	0.17	0.7	0.21

Scoring was done on one cross-section of spinal cord from each animal expressing SOD1<sup>G93A</sup>. In paralyzed mice animals very few motor neurons were left; this affected the low score for the Golgi apparatus, which was scored only in the cell body and not in the processes as Stathmin.

Stathmin scoring: 0, Rare golgi-like stain (same as in normal or WT/hSOD mice); 0.5, occasional grains; 1, some stain in a cell body and an occasional process; 2, intense stain in a cell body and a few processes; 3, more than 50 processes stained per field, one or more cell bodies with intense stain.

Golgi apparatus (GA) scoring: 1, 1 to 2 cells with fragmented GA; 2, 3 to 5 cells with fragmented GA; 3, more than five cells with fragmented GA.

stain (Figure 6),<sup>25</sup> a finding supporting the notion that Golgi fragmentation is not a consequence of apoptosis.

### Abnormal Microtubule Networks in HeLa Cells Expressing Stathmin (Figure 7)

It is virtually impossible to evaluate the networks of neuronal microtubules in sections of paraformaldehyde-fixed spinal cords. To test whether the overexpression of cytoplasmic Stathmin is associated with abnormal microtubules, HeLa cells that were transfected with a Stathmin expression vector were double-immunolabeled for Stathmin and  $\alpha$ -tubulin. In contrast to the well-organized network of microtubules of untransfected cells, cells that overexpressed Stathmin had collapsed or effaced microtubule networks (Figure 7), as reported.<sup>10</sup>

### Expression of Hsp25 in Spinal Cords of Control and Paralyzed Mice (Figure 8)

In contrast to the robust expression of cytoplasmic Hsp25 in spinal cord motor neurons from control mice, the motor neurons of paralyzed mice showed very little or no immunostaining for Hsp25 (Figure 8, first and second panels); in contrast, numerous reactive astrocytes of paralyzed mice contained Hsp25 (Figure 8, second and fourth or bottom panels). In 30-day-old mice, there was no difference in the immunolabeling of Hsp25 between mice expressing the WT and G93A (Figure 8, third panel; 30 days). In contrast, in 90-day-old mice there was a marked decrease in Hsp25 immunolabeling of motor neurons of mutant mice (Figure 8, first panel). Aggregation of mutant SOD1 in astrocytes has been reported in transgenic mice models of fALS and in fALS with SOD1 mutations.<sup>18,19</sup> By double-labeling immunofluorescence, Hsp25 and SOD1 co-localized in the cytoplasm of neurons, in some astrocytes, and in unidentifiable processes of 60-day-old asymptomatic mice expressing the mutant (Figure 9a). In paralyzed mice, reactive astrocytes expressing Hsp25 were found not only in the anterior horn areas, but diffusely throughout the white matter of all columns. The characteristic spidery processes of many reactive astrocytes were immunolabeled with Hsp25, but not with SOD1 (Figure 9b). In paralyzed mice, atrophic cell bodies in the anterior horn areas, presumably of dying motor neurons, displayed immunolabeling of SOD1 and Hsp25 (Figure 9c).

### Co-Precipitation of Hsp25 with SOD1 (Figure 10)

To further examine the possibility of an *in vivo* association of mutant human SOD1 with Hsp25, spinal cord extracts from paralyzed mice and from normal mice expressing WT human SOD1 were immunoprecipitated with an antibody against human SOD1 and the precipitates were immunoblotted with an anti-Hsp25 antibody. This revealed that mutant, but not WT, SOD1 associated with Hsp25 (Figure 10). Western blots of similar immunoprecipitates performed with an anti-Stathmin antibody did not reveal associations between SOD1 and Stathmin (not shown). The specificity of the association between mutant SOD1 and Hsp25 was further confirmed by

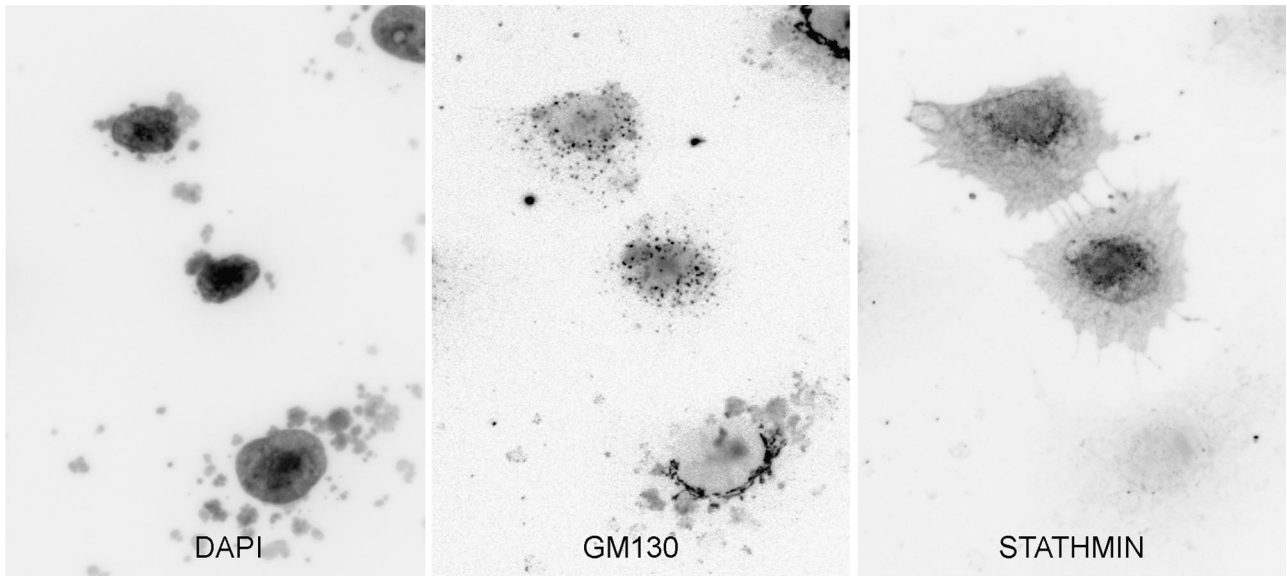


**Figure 6.** HeLa cells transfected with a Stathmin expression vector. Stained for nuclei (DAPI),<sup>23</sup> Golgi apparatus (GM130),<sup>22</sup> and Stathmin.<sup>16</sup> The two cells overexpressing Stathmin have fragmented Golgi apparatus. Original magnifications,  $\times 500$ .

immunoprecipitations with an antibody against Hsp25, or with an irrelevant antibody against the MG160 protein, followed by immunoblotting of the immunoprecipitates with an anti-SOD1 antibody (Figure 10).

#### *Peroxisredoxin 6*

Western blots from homogenates of spinal cords from paralyzed mice and age-matched mice expressing the WT human SOD1 confirmed the significant up-regulation of PRDX6 in paralyzed mice, as initially detected by mass spectroscopy (Figure 11, Table 1). Cross sections of spinal cords from 30-

day-old mice, immunostained with an antibody against PRDX6, showed no difference between controls and mice expressing mutant SOD1 (Figure 12). In contrast an intense and diffuse immunolabeling was seen in astrocytes of paralyzed mice (Figure 12, middle and bottom panels).

#### *Temporal Sequence of Immunocytochemical Observations*

In summary, the following trends were apparent: 1) neuronal Golgi fragmentation was more prominent than

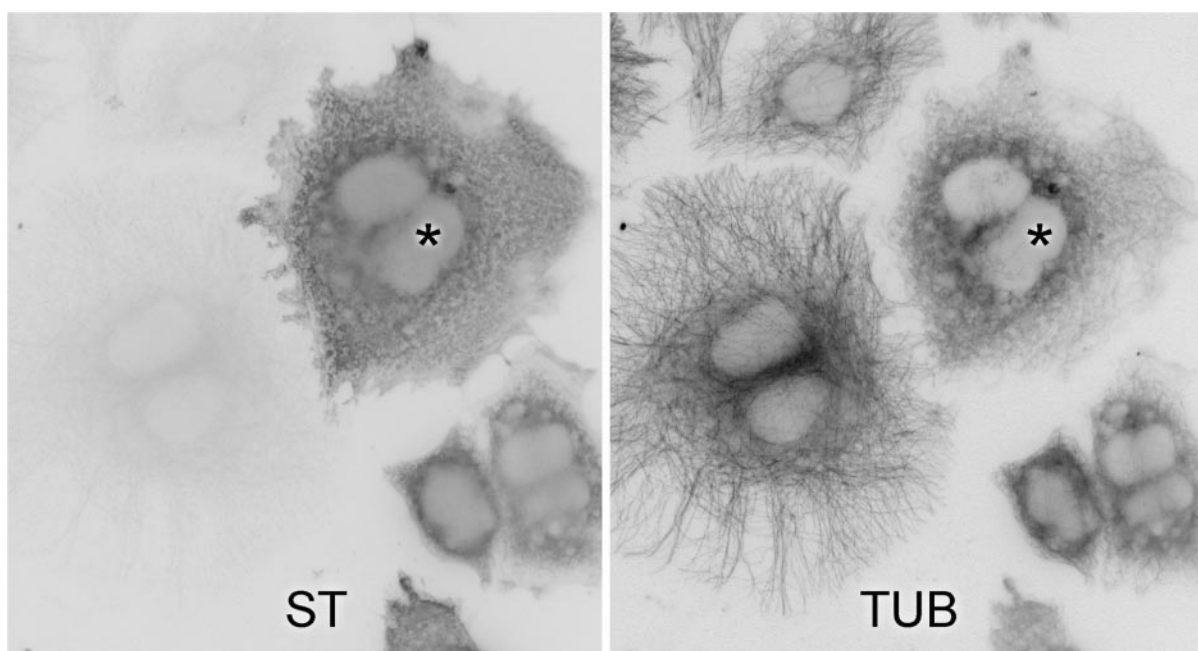


**Figure 7.** HeLa cells transfected with Stathmin were double immunostained for Stathmin (ST) and  $\alpha$ -tubulin (TUB). Compare the intact microtubule network in an untransfected cell to the weak and collapsed network in a cell expressing Stathmin (**asterisk**). Original magnifications,  $\times 600$ .

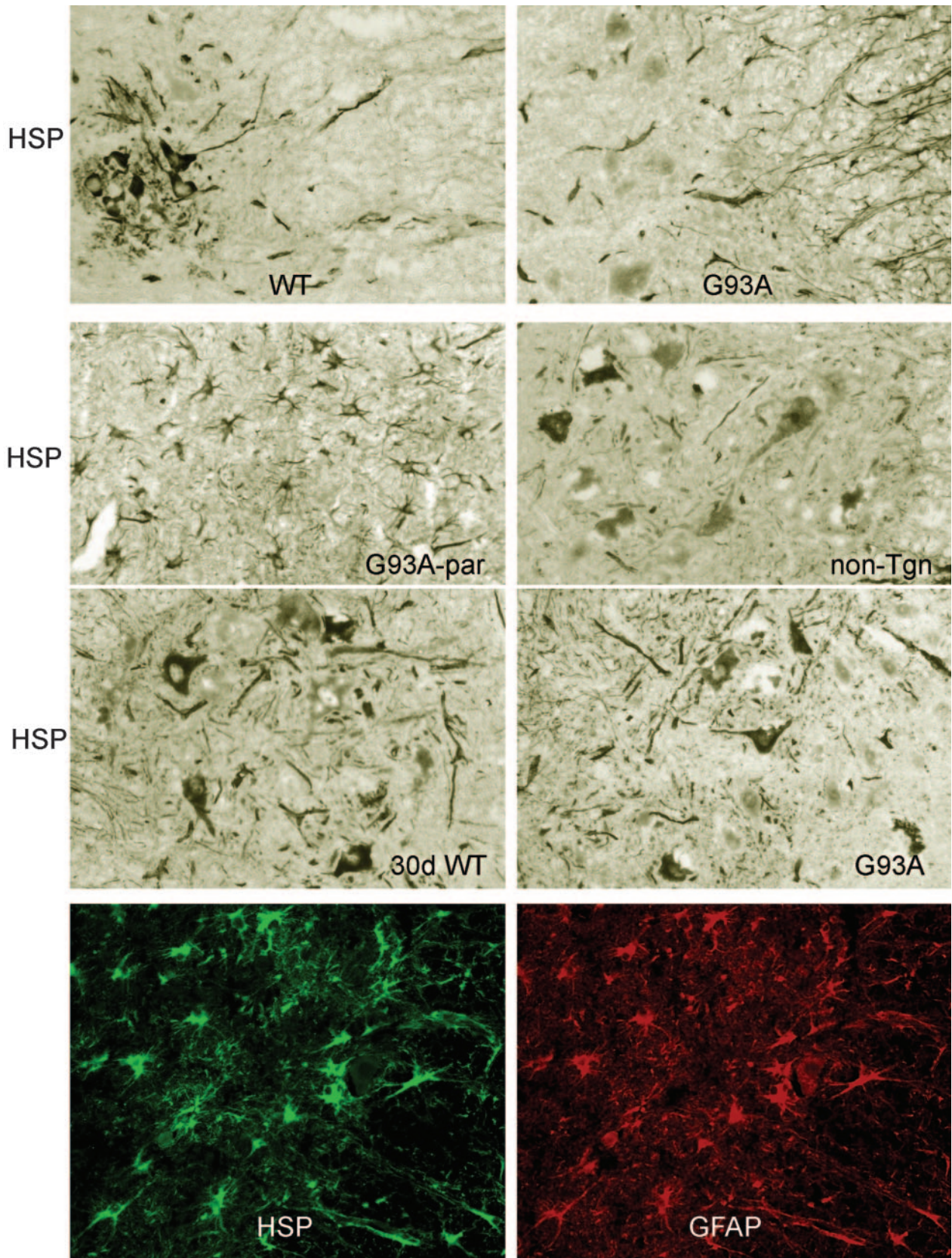


**Figure 8.** Sections of spinal cords immunostained for Hsp25. **First panel:** 90-day-old mice transgenic for WT human SOD1 (WT) or the mutant G93A (G93A). Note weak neuronal cytoplasmic stain. **Second panel:** note stain in astrocytes in paralyzed mouse (G93A-par). The nontransgenic control (non-Tgn) shows Hsp25 in neuronal perikarya. **Third panel:** 30-day-old mouse, transgenic for G93A (30 days G93A) and from control expressing the WT (30 days WT) showing no difference in Hsp25 immunostain. **Fourth and bottom panel:** double immunolabeling for Hsp25 (HSP, green) and GFAP (red) shows Hsp25 accumulation of Hsp in reactive astrocytes. Original magnifications,  $\times 200$ .

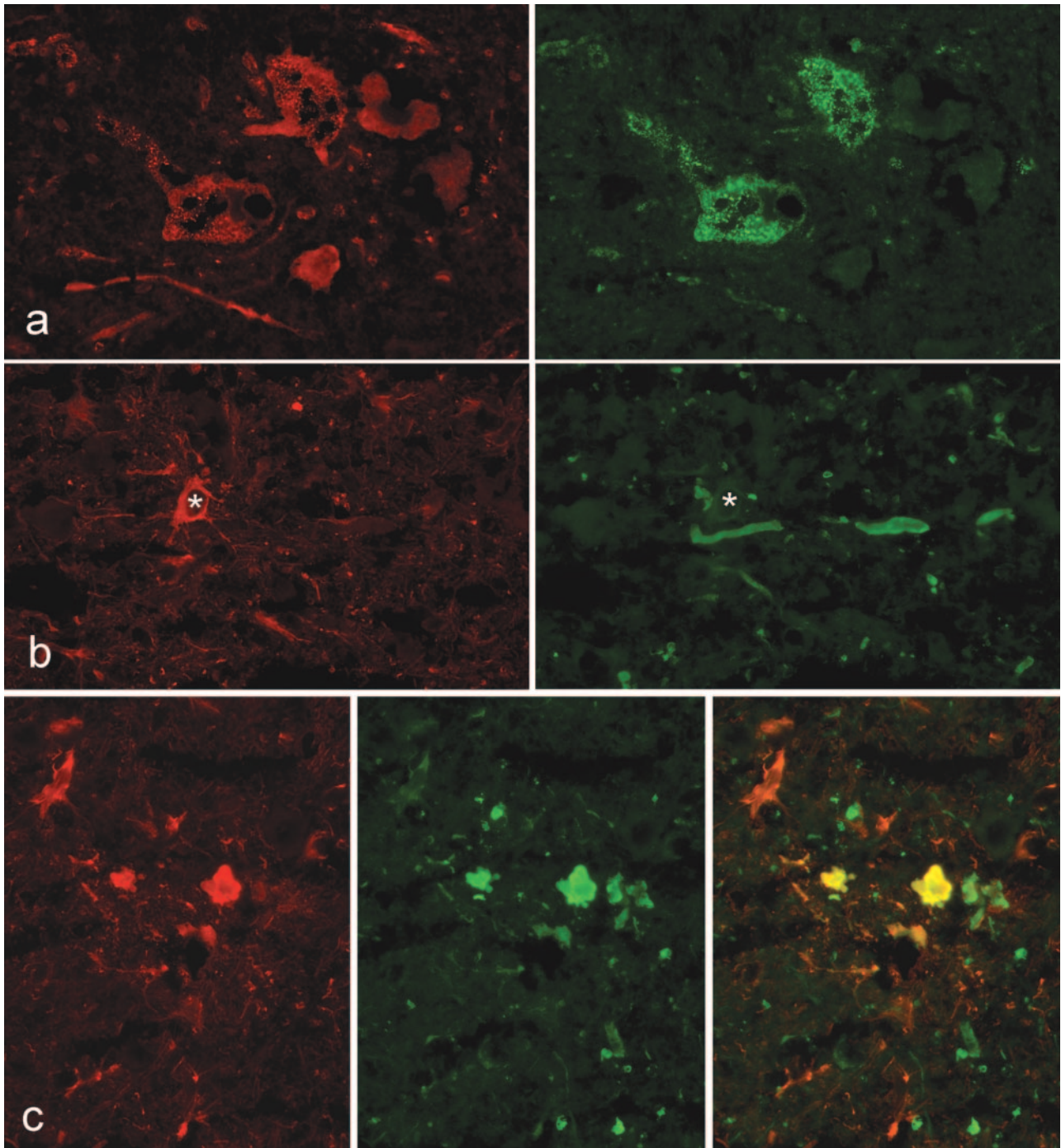


**Figure 9.** Double-immunofluorescence labeling of Hsp25 (**left**) and SOD1 (**right**) in spinal cord sections from mice expressing SOD1<sup>G93A</sup>. **a:** Sixty-day-old mouse. Expression of both Hsp25 and SOD1 in neurons. **b:** Paralyzed mouse. Most reactive astrocytes (**asterisk**) express only Hsp25. **c:** Paralyzed mouse. Anterior horn area. **Left,** Hsp25; **middle,** SOD1; **right,** merge showing double labeling of probably dying neurons. Original magnifications:  $\times 200$  (**a**);  $300$  (**b**);  $400$  (**c**).

Stathmin accumulation in 60- to 90-day-old mice that expressed mutant SOD1 (Table 2). Stathmin did not co-localize with SOD1 (not shown). 2) In 60-day-old mice neuronal perikarya were stained for Hsp25, but slightly less than controls, and there was a slight increase of Hsp25 staining in astrocytes. SOD1 was present in neuronal perikarya and processes. 3) In 90-day-old mice (Figure 8), there was less Hsp25 in the decreased number of motor neurons, whereas astrocytic Hsp25 staining

increased. Intense SOD1 stain was present in cell bodies and processes. 4) In paralyzed mice (Figure 8), an intense staining of Hsp25 was found in an increased number of reactive astrocytes. Hsp25 co-localized with SOD1 in processes, and in occasional astrocytes and neurons. 5) There was no difference in neuronal and glial stain for PRDX6 between 30-day-old mice that expressed WT or mutant SOD1. In paralyzed mice all reactive astrocytes expressed PRDX6 (Figure 12).

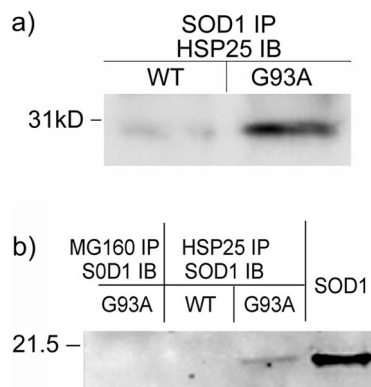


**Figure 10.** Immunoprecipitations: extracts from five pooled spinal cords from symptom-free mice expressing the WT, and paralyzed mice expressing the mutant (G93A), were immunoprecipitated with **a:** an anti-SOD1 antibody, followed by immunoblotting with an antibody against Hsp25; **b:** Immunoprecipitations with an irrelevant antibody (MG160 IP) followed by immunoblotting with an anti-SOD1 antibody, or immunoprecipitations with an anti-Hsp25 antibody followed by immunoblotting with an anti-SOD1 antibody; SOD1 standard = bovine red blood cell SOD1.

## Discussion

Protein profiling of spinal cord homogenates from paralyzed transgenic mice expressing SOD1<sup>G93A</sup> compared to that of 6- to 8-week-old asymptomatic mice that expressed the same mutant and controls (age-matched transgenic mice expressing the WT human SOD1) revealed a significant, selective, and so far not reported, down-regulation of one isoform of the microtubule depolymerizing Stathmin (Figure 3, b and c), and an up-regulation of Hsp25, Hsp27, phosphatidylinositol transfer protein- $\alpha$ , apolipoprotein E, ferritin heavy chain, and of the anti-oxidant PRDX6 (Table 1). The up-regulation of Hsp25 and Hsp27 in the spinal cords of paralyzed mice expressing SOD1<sup>G93A</sup> was reported in cultured cells expressing SOD1 mutants (Figures 1 and 2 and Table 1).<sup>17</sup>

Changes of low-abundance proteins may escape detection in protein profiling performed in homogenates of the entire spinal cord. Future protein profiling studies in subcellular fractions, such as the Golgi apparatus, high-speed supernatants, and mitochondria, may reveal changes of low-abundance proteins that are normally enriched in these fractions. The mouse model of fALS is ideal for these studies because tissues can be obtained without damage because of postmortem autolysis, which is not possible in autopsy tissues from human ALS.

## Stathmin

We examined a possible role of Stathmin in the pathogenesis of mutant SOD1 toxicity for the following reasons:

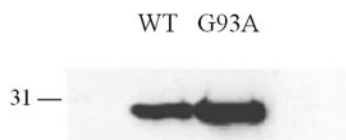


**Figure 11.** Western blots from five pooled spinal cord extracts from age-matched transgenic mice expressing the WT, and paralyzed mice expressing the mutant (G93A), probed with an antibody against PRDX6.<sup>23,34</sup>

1) the known microtubule destabilizing activity of Stathmin;<sup>8-10</sup> 2) the dependence of the structure of the Golgi apparatus on intact microtubules;<sup>11,12</sup> 3) the fragmentation of the organelle by microtubule depolymerizing drugs<sup>11,12</sup> in transgenic mice expressing SOD1<sup>G93A</sup>, in fALS with SOD1 mutations, and in sporadic ALS.<sup>13,14</sup>

Most probably, mutant SOD1 sets in motion a series of reactions involving the posttranslational modification of the most acidic phosphoisoform of Stathmin (Figure 3c). This was associated with the cytoplasmic accumulation of Stathmin and the proteins of the same family SCLIP and SCG10 (Figure 4, G93A), and the fragmentation of the Golgi apparatus of all neurons with Stathmin accumulations (Figure 5). *In vitro* experiments with HeLa cells overexpressing Stathmin showed Golgi fragmentation and the disruption of microtubule networks (Figures 6 and 7). These results suggest that *in vivo*, Stathmin contributes to the fragmentation of the Golgi apparatus. Additional work needs to be done to establish whether and how mutant SOD1 affects other phosphoproteins, *in vivo* and in cultured cells, and whether the selective reduction of the most acidic and heavily phosphorylated isoform of Stathmin is the cause or consequence of Golgi fragmentation in this mouse model of fALS.<sup>10</sup>

Stathmin and SCLIP and SCG10, members of the same family of regulatory phosphoproteins, are wide spread through a variety of tissues and play important roles in the homeostasis of microtubules.<sup>8-10</sup> Although Stathmin is soluble, the two phosphoproteins of the same family, SCG10 and SCLIP, are bound to membranes of the Golgi apparatus.<sup>8-10</sup> Stathmin, SCG10, and SCLIP are enriched in the central nervous system and especially in neurons.<sup>8</sup> Stathmin is 2 to 50 times more abundant in most neonatal mouse tissues in comparison to adult tissues.<sup>24</sup> The neonate mouse central nervous system contains 9 to 10 times the adult levels of Stathmin.<sup>24</sup> The activities of these proteins are complex and most likely are involved in both developmental regulations in the embryo and young animals, and in functional regulations in the adult, mostly in the central nervous system.<sup>24</sup> Stathmin is uniformly present in the neuronal cell body, dendrites, axons, and growth cones.<sup>9</sup> Overexpression of wild-type and phosphorylation site mutants of Stathmin suggests that nonphosphorylated Stathmin induces the depolymerization of interphase and mitotic microtubules.<sup>10</sup> In that regard it is important to note that the reduction in paralyzed mice of the most acidic phosphorylated isoform of Stathmin and the decreased immunostaining with antisera against the phosphorylation sites 16, 25, and 38 might provide an explanation for microtubule depolymerization and Golgi fragmentation (Figure 3c). Quantitative studies are required to establish whether Stathmin phosphoforms are differentially regulated in the paralyzed mice and involved in the depolymerization of microtubules and Golgi fragmentation. *In vitro* experiments, however, strongly suggest that Stathmin overexpression is associated with abnormal microtubules and Golgi fragmentation (Figures 6 and 7), just as in spinal cord sections from paralyzed mice in which Golgi fragmentation was associated with Stathmin accumulation (Figures 4 and 5).

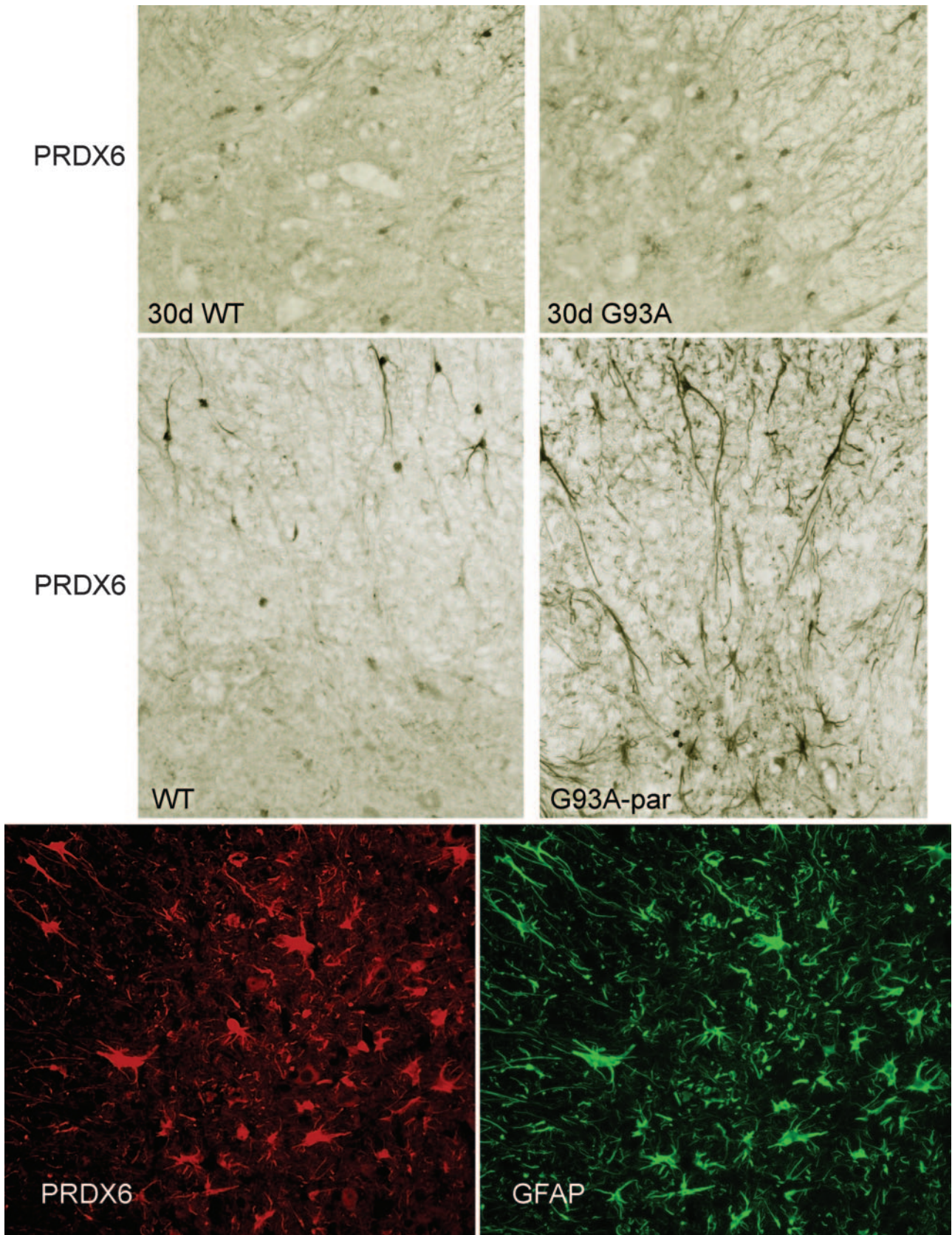


**Figure 12.** Spinal cord sections immunostained with an anti-PRDX6 antibody. **Top:** 30-day-old mice expressing the WT or the mutant (G93A). **Middle:** Age-matched mouse expressing the WT (WT) and paralyzed mouse expressing the mutant (G93A). Note staining of astrocytes and processes in G93A. **Bottom:** Double labeling with an antibody against PRDX6 (red) and GFAP (green). Reactive astrocytes are labeled by PRDX6. Original magnifications,  $\times 200$ .

The issue of the Stathmin isoform(s) that accumulate in neurons and processes (Figure 4), and the mechanism of its activation in spinal cord motor neurons with fragmented Golgi apparatus of paralyzed mice expressing mutant SOD1 is an important one. It should be stated, however, that mutant SOD1 does not co-localize or co-precipitate with Stathmin in immunoprecipitations that were performed in homogenates of the entire spinal cord (not shown). The decrease of only one isoform of Stathmin, detected by immunoblots of two-dimensional gels (Figure 3c), confirms a similar decrease detected by two-dimensional gels and protein staining, in which only one spot showing a significant change from the WT control was subsequently sequenced (Figure 2) (Table 1). The accumulation of Stathmin, SCLIP, and SCG10 in the cytoplasm of many degenerating motor neurons of paralyzed mice expressing SOD1<sup>G93A</sup>, detected by immunocytochemistry, is impressive and never seen in sections from control mice expressing the WT human SOD1, or in age-matched normal controls (Figure 4).

Unlike Hsp25 (Figure 3a), Stathmin, does not aggregate in detergent insoluble fractions (Figure 3b). The association of fragmented Golgi apparatus in neurons with accumulation of cytoplasmic Stathmin suggests a causal linkage between the disruption of the structure of the organelle and Stathmin accumulation (Figures 4 and 5). This hypothesis is supported by the experimental evidence of abnormal microtubule networks and fragmented Golgi apparatus in HeLa cells that overexpressed Stathmin (Figures 6 and 7). It is noteworthy, however, that double labeling of Stathmin and SOD1 in spinal cord sections from paralyzed mice rarely showed co-localization of Stathmin with SOD1, and co-precipitation experiments did not show an association between SOD1 and Stathmin (not shown). In contrast to Stathmin, Hsp25 co-precipitated with SOD1 (Figure 10).

The emergence of the microtubule-depolymerizing protein Stathmin as a possible factor or mediator of mutant SOD1 toxicity in this mouse model is consistent with a recent report that the levels of the microtubule-stabilizing proteins MAP2, MAP1, tau 100 kd, and tau 68 kd decreased 5 months before the onset of symptoms in SOD1<sup>G37R</sup> mice.<sup>39</sup> Therefore, it would be interesting to examine in transgenic mice that express mutants of SOD1 whether the decrease of Stathmin precedes, coincides, or follows the decrease of the microtubule-stabilizing proteins.

### *Stathmin in Other Neurodegenerative Disorders*

Stathmin-deficient mice developed an age-dependent central and peripheral axonopathy with a clinical phenotype similar to that of ALS.<sup>40</sup> The concentration of Stathmin was reduced in the neocortex of patients with Alzheimer's disease, whereas Stathmin aggregated in some neurons with neurofibrillary tangles.<sup>41</sup> Interestingly, certain neurons in Alzheimer's disease have fragmented Golgi apparatus.<sup>42</sup> A similar reduction of brain Stathmin was reported in Down's syndrome and in Alzheimer's disease.<sup>43</sup> These reports suggest that Stathmin may play

the role of a second toxic messenger in the pathogenesis of neurodegeneration in fALS with SOD1 mutations and in other neurodegenerative diseases.

### *Golgi Fragmentation and Mutant SOD1*

The cause(s) and significance of Golgi fragmentation in ALS and in transgenic mice expressing SOD1<sup>G93A</sup> are not known. The occurrence of Golgi fragmentation in spinal cord motor neurons of transgenic mice expressing SOD1<sup>G93A</sup>, months before the onset of paralysis, indicates that it is an early reaction.<sup>15</sup> The proximity of aggregates of SOD1<sup>G93A</sup> to fragmented elements of the GA suggests that mutant protein may affect one or more proteins involved in the structural organization of the organelle.<sup>44</sup> It was also proposed that the aggregation of mutant SOD1 in detergent insoluble fractions was linked to toxicity.<sup>45</sup> However, the formation of cytoplasmic aggregates of mutant SOD1 protein may not be required for an initial trigger of motor neuron death; aggregates of mutant SOD1 may either cause ALS, or represent correlates or consequences of mutant SOD1 toxicity.<sup>46</sup>

To gain insights into the significance of Golgi fragmentation, we developed an experimental model of mutant SOD1 toxicity in CHO cells expressing the enzymatically active G93A or the inactive G85R mutant. Cells expressing either of the two mutants showed Golgi fragmentation, decreased viability, and compromised function of the secretory pathway. Moreover, the formation of cytoplasmic inclusions by mutant protein was not required for toxicity.<sup>47</sup> These results re-emphasize the role of the Golgi apparatus in the pathogenesis of the disease and challenges the notion that the aggregation of mutant protein in inclusion bodies is a requirement for toxicity.

### *Golgi Fragmentation in Parkinson's Disease*

A recent study on the mechanisms of neuronal degeneration in Parkinson's disease placed particular emphasis on the fragmentation of the Golgi apparatus and the subsequent impairment of protein trafficking.<sup>48</sup> The authors suggested that the fibrillar inclusion bodies in Parkinson's disease were consequences rather than causes of toxicity and presented evidence supporting the notion that the prefibrillar aggregates of  $\alpha$ -synuclein are the pathogenetic species affecting specifically the Golgi apparatus and protein trafficking.

### *Golgi Fragmentation by Misfolded Truncated Growth Hormone*

In certain individuals with an isolated, autosomal dominant growth hormone deficiency, one copy of the growth hormone lacks amino acids 32 to 71 and is misfolded.<sup>49</sup> The expression of the truncated hormone in COS7 cells was associated with Golgi fragmentation, absence of the microtubule organizing centers, and impaired protein trafficking.<sup>49</sup>

### *Golgi Fragmentation and Nonapoptotic Death in Astrocytes Expressing the Tau Protein*

Several human neurodegenerative disorders, including Alzheimer's disease, are associated with aggregated tau proteins in neurons and astrocytes. The overexpression of the longest isoform of human tau in primary cultures of rat astrocytes resulted in the fragmentation of the Golgi apparatus and nonapoptotic cell death.<sup>50</sup> This finding suggests that Golgi fragmentation may mediate cell death by nonapoptotic mechanisms.

In summary, the fragmentation of the Golgi apparatus, originally discovered in sporadic ALS,<sup>13</sup> and confirmed in transgenic mice expressing SOD1<sup>G93A</sup>, is not restricted to ALS.<sup>15</sup> An identical lesion of the organelle has been reported in cells expressing mutant  $\alpha$ -synuclein, truncated growth hormone, or the tau protein.<sup>48–50</sup> This fragmentation is probably caused by a variety of mechanisms involving the homeostasis of microtubules,<sup>12</sup> Golgi matrix proteins,<sup>22</sup> and trafficking. Misfolded or overexpressed normal proteins, such as tau, may modulate the homeostasis of microtubules.

### *Hsp25*

Several small heat shock proteins, including Hsp25, interact with nonnative proteins, prevent their aggregation and promote their refolding.<sup>51</sup> Hence, the up-regulation of Hsp25 in spinal cords of transgenic mice with aggregates of SOD1<sup>G93A</sup> is not surprising.<sup>44,45</sup> However, the apparent down-regulation of Hsp25 in motor neurons and its simultaneous up-regulation in reactive astrocytes of paralyzed mice is novel and intriguing (Figure 9). The differential modulation of Hsp25 in neurons and astrocytes is not unique to the SOD1<sup>G93A</sup> mouse model of fALS. A similar differential regulation of Hsp25 was reported in a spontaneous mutation in mice involving the degeneration and death of anterior horn motor neurons.<sup>52</sup> Another small heat shock protein,  $\alpha$ B crystallin is associated with tau inclusions in glia suggesting that small Hsps react to a variety of misfolded proteins.<sup>53</sup>

The co-precipitation of mutant SOD1 with Hsp25 (Figure 10) was reported in a cultured neuronal cell line model of mutant SOD1 toxicity.<sup>17</sup> Therefore, evidence from this mouse model and a cell culture model of fALS strongly suggest that Hsp25 is involved in the pathological process. This may be an important consequence of mutant SOD1 toxicity because the mutant protein by co-precipitating with Hsp25 may deprive cells of the anti-apoptotic and other protective effects of Hsp25.<sup>17</sup>

Dorfin, a RING finger-type ligase for mutant SOD, reduced the amount of mutant SOD1 in mitochondria, the release of cytochrome c, and caspase activation.<sup>54</sup> However, unlike Hsp25, there was no information that Dorfin co-precipitated with mutant SOD1.<sup>54</sup>

### *Peroxiredoxin 6*

The anti-oxidant protein PRDX6, or anti-oxidant protein 2 (AOP2), is a member of a family of thiol-specific antioxi-

dants, recently renamed peroxiredoxins. These proteins evolved as a part of a system to counteract the damaging effects of oxygen radicals. Peroxiredoxin 6 was found in the cytosol of endothelial cells, erythrocytes, and monocytes, but not in granulocytes.<sup>23</sup> The present study has disclosed, for the first time, a possible role of PRDX6 in the central nervous system in a mutant SOD1-linked model of fALS. The so-far unique up-regulation of PRDX6 in paralyzed mice expressing SOD1<sup>G93A</sup> (Figures 11 and 12) needs to be confirmed in human ALS, especially because "PRDX6 is a unique nonredundant antioxidant that functions independently of other peroxiredoxins and antioxidant proteins."<sup>34</sup> It is intriguing that PRDX6 showed a significant up-regulation in the frontal cortex of patients with Parkinson's disease, and down-regulation in parkin-deficient mice.<sup>55,56</sup> The up-regulation of PRDX6 in the spinal cords of paralyzed SOD1<sup>G93A</sup> mice probably represents a defensive compensatory reaction to the oxidative damage to a variety of substrates in ALS and in mutant SOD1-mediated disease.<sup>57</sup>

### *Gene Expression and Proteomic Analyses in Models of Amyotrophic Lateral Sclerosis*

To gain insights into possible molecular targets of mutant SOD1, several investigators have exploited gene expression profiling or proteome analysis. None of these studies, however, brought into focus Stathmin, Hsp25, or PRDX6. Differences in the choices of tissues and methods, or in the disease stage may be responsible for this lack of consistency. Furthermore the weak correlation of abundance revealed by transcriptome or proteome analyses could also account for the so far unrecognized roles of Stathmin, Hsp25, and PRDX6 in mutant SOD1 toxicity.<sup>58</sup>

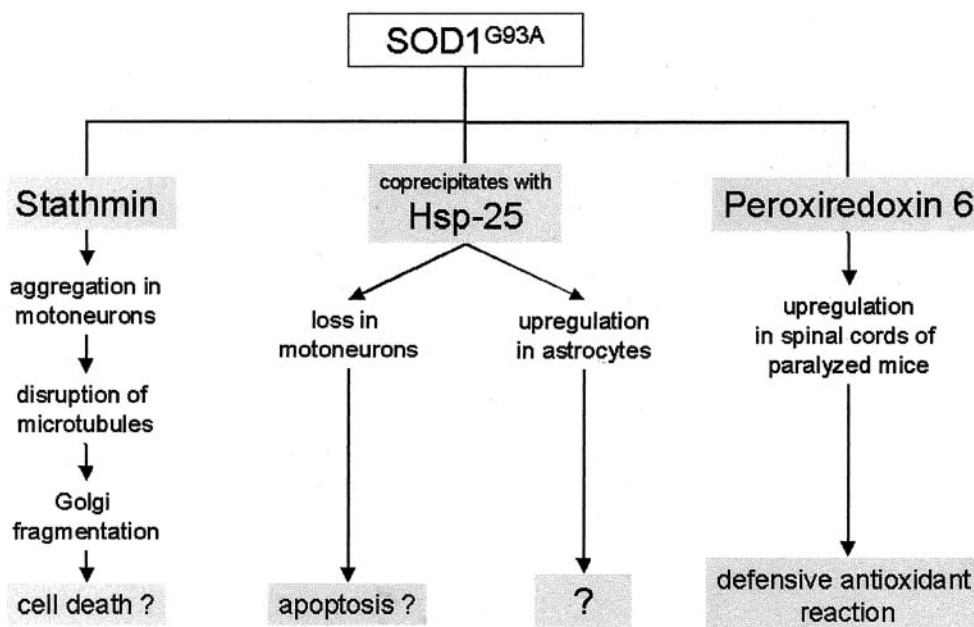
Transcription profiling in spinal cords of transgenic mice expressing the G93A mutant of SOD1 disclosed activation of genes involved in metal ion regulation.<sup>59</sup> A similar study revealed a differential expression of inflammation- and apoptosis-related genes.<sup>60</sup> Genes involved in vesicular trafficking and apoptosis were differentially regulated in cultured cells expressing the G37R, G93A, or I113T mutants.<sup>61</sup> Cytosolic proteome analysis in cultured cells expressing the mutants G37R or G93A, and laser capture microdissection of spinal cord motor neurons from human fALS, implicated proteins involved in antioxidant defenses, proteasome function, and nitric acid metabolism.<sup>62</sup>

Four of the fourteen genes that were differentially expressed in spinal cords from human sporadic ALS, have antioxidant properties. Of these, three were up-regulated, ie, thioredoxin, lysyl oxidase, and flavin containing monooxygenase, and one, a flavin-containing mono-oxygenase 1, was down-regulated.<sup>63</sup>

### *Cell Synergy Is Required for Disease Development*

The aggregation of mutant protein in astrocytes and oligodendrocytes of transgenic mice expressing SOD1 mu-

**Table 3.** Suggested Pleiotropic Actions of Mutant SOD1



tants suggests that neurons are not the exclusive targets in this model of fALS.<sup>18,19,64</sup> This hypothesis has received additional support from experiments with transgenic mice that were symptom-free when mutant SOD1 was expressed only in neurons<sup>65,66</sup> or in astrocytes.<sup>67</sup> Furthermore, in chimeric mice containing mixtures of normal and SOD1 mutant-expressing cells, toxicity to motor neurons and aspects of ALS pathology depended on nonneuronal cells.<sup>68</sup> Therefore, the overexpression of Hsp25 and PRDX6 in astrocytes may contribute to or represent defenses against SOD1 toxicity.

Suggested pleiotropic actions of mutant SOD1, summarized in Table 3, indicate the involvement of Stathmin, Hsp25, and PRDX6 in the pathogenesis of the disease. Most likely, mutant SOD1 sets in motion reactions that involve Stathmin, Hsp25, Hsp27, PRDX6, and other proteins as well. It remains to be determined whether these differential regulations are independent of each other or they represent interdependent and tightly controlled sequential reactions. Future therapeutic approaches in ALS may have to be targeted on a variety of protein systems.

In summary, the involvement of Hsp25 in mutant SOD1 toxicity confirms a study in a cultured neuronal line.<sup>17</sup> The mouse model, however, showed that Hsp25 is differentially expressed in reactive astrocytes and motor neurons (Figure 8). This deserves further investigation. The coprecipitation of Hsp25 with mutant SOD1 (Figure 10) is consistent with the hypothesis that mutant SOD1 toxicity is mediated, at least in part, by the deprivation of cells of the anti-apoptotic and other protective activities of Hsp25.<sup>17</sup>

The so-far unique up-regulation of the antioxidant PRDX6, may be a compensatory response to oxidant damage. If that is the case, the expression of a SOD1

mutant in PRDX6<sup>-/-</sup> mice<sup>34</sup> may aggravate the course of the disease, and conversely the overexpression of PRDX6 in mice with a SOD1 mutation may improve the course of the disease. The generation of appropriate double mutants may offer a unique opportunity to test the role of PRDX6 in modulating the disease in transgenic mice expressing a mutant SOD1. The development of a drug-mimetic or -enhancing PRDX6, and its application in SOD1 mutant mice may test the efficacy of treatment of fALS with SOD1 mutations with a native antioxidant that is up-regulated during the course of the disease in transgenic mice expressing SOD1<sup>G93A</sup>.

The involvement of the microtubule depolymerizing protein Stathmin in the pathogenesis of this mouse model of familial ALS (SOD1<sup>G93A</sup>) is novel and of potential interest because it may offer a molecular explanation for the fragmentation of the Golgi apparatus observed in sporadic ALS, in fALS with SOD1 mutations, and in transgenic mice expressing SOD1<sup>G93A</sup>.<sup>13-15</sup> Golgi fragmentation has also been associated with an  $\alpha$ -synucleinopathy of Parkinson's disease,<sup>48</sup> with misfolded truncated growth hormone,<sup>49</sup> and in a tau-mediated death of astrocytes.<sup>50</sup> Therefore, it is reasonable to suggest that a variety of misfolded proteins share common pathogenic mechanisms affecting microtubules, the Golgi apparatus, and protein trafficking. It remains to be proven whether Stathmin is a common mediator of these toxic reactions.

### Acknowledgments

We thank Dr. Mike W. Winters for his suggestions in mass spectroscopy; Dr. Lanfang Xu in two-dimensional gel

electrophoresis; Dr. A. Sobel, INSERM, Paris, France, for antibodies against SCG10, SCLIP, and the Stathmin phosphoforms, S16P2, S25P2, S38P2,<sup>8-10</sup> and many useful suggestions; and Dr. Donna George (University of Pennsylvania, Philadelphia, PA) for the cDNA for human Stathmin.<sup>28</sup>

## References

- Hirano A: Cytopathology of amyotrophic lateral sclerosis: a personal perspective of recent developments. *Neuropathology* 1995, 15:1-6
- Kondo K: Epidemiological aspects of motor neuron disease. *Amyotrophic Lateral Sclerosis: Progress and Perspectives in Basic Research and Clinical Application*. Edited by P Nakano, A Hirano. Amsterdam, Elsevier Excerpta Medica, International Congress Series 1996, 1104, pp 133-141
- Okumura H, Chen K-M, Kurland LT: Recent epidemiological study of ALS and PDC in Guam Island. *Amyotrophic Lateral Sclerosis: Progress and Perspectives in Basic Research and Clinical Application*. Edited by P Nakano, A Hirano. Amsterdam, Elsevier Excerpta Medica, International Congress Series 1996, 1104, pp 154-157
- Deng HX, Hentati A, Tainer JA, Iqbal Z, Cayabyab A, Hung WY, Getzof ED, Hu P, Herzfeld B, Roos RP, Warner C, Deng G, Soriano E, Smyth C, Parge HE, Ahmed A, Roses AD, Hallewell RA, Pericak-Vance MA, Siddique T: Amyotrophic lateral sclerosis and structural defects in Cu, Zn superoxide dismutase. *Science* 1993, 261:1047-1051
- Rosen DR, Siddique T, Patterson S, Figlewicz DA, Sa P, Hentati A, Donaldson D, Goto J, O'Reagan JP, Deng HX, Rahmani Z, Krizus A, McKenna-Yasek D, Cayabyab A, Gaston SM, Berger R, Tanzi RE, Halperin JJ, Herzfeldt B, Van den Bergh R, Hung WY, Bird T, Deng G, Mulder DW, Smyth C, Laing NG, Soriano E, Pericak-Vance MA, Haines J, Rouleau GA, Gusella GS, Horvitz HR, Brown Jr RH: Mutations in Cu/Zn superoxide dismutase gene are associated with familial amyotrophic lateral sclerosis. *Nature* 1993, 362:59-62
- Gurney ME, Pu H, Chiu AY, Chiu DCM, Dal Canto MC, Polchow CY, Alexander DD, Caliendo J, Hentati A, Kwon YW, Deng H-X, Chen W, Zhai P, Sufit RL, Siddique T: Motor neuron degeneration in mice that express a human Cu, Zn superoxide mutation. *Science* 1994, 264:1772-1775
- Julien, J-P: Review. Amyotrophic lateral sclerosis: unfolding the toxicity of the misfolded. *Cell* 2001, 104:581-591
- Sobel A, Butterin M-C, Beretta L, Chneiweis H, Doye V, Peyro-Saint-Paul H: Intracellular substrates for extracellular signaling. Characterization of a ubiquitous, neuron enriched phosphoprotein (Stathmin). *J Biol Chem* 1989, 264:3765-3772
- Gavet O, Messari SE, Ozon S, Sobel A: Regulation and subcellular localization of the microtubule-destabilizing Stathmin family phosphoproteins in cortical neurons. *J Neurosci Res* 2002, 68:535-550
- Gavet O, Ozon S, Manceau V, Lawler S, Curmi P, Sobel A: The Stathmin phosphoprotein family: intracellular localization and effects on the microtubule network. *J Cell Sci* 1998, 111:3333-3346
- Robbins E, Gonatas NK: Histochemical and ultrastructural studies on HeLa cell cultures exposed to spindle inhibitors with special reference to the interphase cell. *J Histochem Cytochem* 1964, 1:704-711
- Kreis TE, Goodson HV, Perez F, Roonholm R: Golgi apparatus-cytoskeleton interactions. *The Golgi Apparatus*. Edited by EG Berger, J Roth. Basel, Birkhauser, 1997:179-193
- Gonatas NK: Contributions to the physiology and pathology of the Golgi apparatus. *Am J Pathol* 1994, 145:751-761
- Fujita Y, Okamoto K, Sakurai A, Gonatas NK, Hirano A: Fragmentation of the Golgi apparatus of the anterior horn cells in patients with familial amyotrophic lateral sclerosis with SOD1 mutations and posterior column involvement. *J Neurol Sci* 2000, 174:137-140
- Mourelatos Z, Gonatas NK, Stieber A, Gurney ME, Dal Canto MC: The Golgi apparatus of spinal cord motor neurons in transgenic mice expressing mutant Cu, Zn superoxide dismutase becomes fragmented in early, preclinical stages of the disease. *Proc Natl Acad Sci USA* 1996, 93:5472-5477
- Tu PH, Gurney MC, Julien J-P, Lee M-Y V, Trojanowski JQ: Oxidative stress, human SOD1, and neurofilament pathology in transgenic mouse models of human motor neuron disease. *Lab Invest* 1997, 76:441-456
- Okado-Matsumoto A, Fridovich I: Amyotrophic lateral sclerosis: a proposed mechanism. *Proc Natl Acad Sci USA* 2002, 99:9010-9014
- Brujin LI, Becher MW, Lee MK, Anderson KL, Jenkins JA, Copeland NG, Sisodia SS, Rothstein JD, Borchelt DR, Price DL, Cleveland DW: ALS-linked SOD1 mutant G85R mediates damage to astrocytes and promotes rapidly progressive disease with SOD1-containing inclusions. *Neuron* 1997, 18:327-338
- Kato S, Shimoda M, Watanabe Y, Nakashima K, Takahashi K, Ohama E: Familial amyotrophic lateral sclerosis with a two base pair deletion in superoxide dismutase 1 gene: multisystem degeneration with intracytoplasmic inclusions in astrocytes. *J Neuropathol Exp Neurol* 1996, 55:1089-1101
- Gonatas JO, Mezitis SGE, Stieber A, Fleischer B, Gonatas NK: MG-160. A novel sialoglycoprotein of the medial cisternae of the Golgi apparatus. *J Biol Chem* 1989, 264:646-653
- Croul S, Mezitis SGE, Stieber A, Chen Y, Gonatas JO, Goud B, Gonatas NK: Immunocytochemical visualization of the Golgi apparatus in several species, including human, and tissues with an antiserum against MG-160, a sialoglycoprotein of rat Golgi apparatus. *J Histochem Cytochem* 1990, 38:957-963
- Lowe M, Gonatas NK, Warren G: The mitotic phosphorylation cycle of the cis-Golgi matrix protein GM130. *J Cell Biol* 2000, 149:341-355
- Stuhlmeier KM, Kao J, Wallbrandt P, Lindberg M, Hammarstrom B, Broell H, Paigen B: Antioxidant protein 2 prevents methemoglobin formation in erythrocyte hemolysates. *Eur J Biochem* 2003, 270:334-341
- Koppel JJ, Butterin M-C, Doye V, Peyro-Saint-Paul H, Sobel A: Developmental tissue expression and phylogenetic conservation of Stathmin, a phosphoprotein associated with cell regulations. *J Biol Chem* 1990, 265:3703-3707
- Collins J, Schandl CA, Young KK, Vessely J, Willingham MC: Major DNA fragmentation is a late event in apoptosis. *J Histochem Cytochem* 1997, 45:923-934
- Stieber A, Gonatas JO, Collard J-F, Meier J, Julien J-P, Schweitzer P, Gonatas NK: The neuronal Golgi apparatus is fragmented in transgenic mice expressing a human SOD1, but not in mice expressing the human NF-H gene. *J Neurol Sci* 2000, 173:63-67
- Johnston PA, Stieber A, Gonatas NK: A hypothesis on the traffic of MG160, a medial Golgi sialoglycoprotein, from the trans-Golgi network to the Golgi cisternae. *J Neurol Sci* 1994, 107:529-537
- Ahn J, Murphy M, Kratowicz S, Wang A, Levine AJ, George D: Down-regulation of the Stathmin/Op28 and FKBR genes following p53 induction. *Oncogene* 1999, 18:5954-5958
- Gonatas JO, Chen Y-J, Stieber A, Mourelatos Z, Gonatas NK: Truncations of the C-terminal cytoplasmic domain of MG160, a medial Golgi sialoglycoprotein, result in its partial transport to the plasma membrane and filopodia. *J Cell Sci* 1998, 111:249-260
- Bradford MM: A rapid and sensitive method for the quantitation of microgram quantities of protein utilizing the principle of protein-dye binding. *Anal Biochem* 1976, 72:248-254
- Langen H, Roder D, Juranville JF, Fountoulakis M: Effect of protein application mode and acrylamide concentration on the resolution of protein spots separated by two-dimensional gel electrophoresis. *Electrophoresis* 1997, 18:2085-2090
- Alb Jr JG, Cortese JD, Phillips SE, Albin RL, Nagy TR, Hamilton BA, Bankaitis VA: Mice lacking phosphatidylinositol transfer protein-alpha exhibit spinocerebellar degeneration, intestinal and hepatic steatosis, and hypoglycemia. *J Biol Chem* 2003, 278:33501-33518
- Haasdijk ED, Vlug A, Mulder MT, Jaarsma D: Increased apolipoprotein E expression correlates with the onset of neuronal degeneration in the spinal cord of G93A-SOD1 mice. *Neurosci Lett* 2002, 335:29-33
- Wang X, Phelan SA, Forsman-Semb K, Taylor EF, Petros C, Brown A, Lerner CP, Paigen B: Mice with targeted mutation of peroxiredoxin 6 develop normally but are susceptible to oxidative stress. *J Biol Chem* 2003, 278:25179-25190
- Double KL, Gerlach M, Youdim MB, Riederer P: Impaired iron homeostasis in Parkinson's disease. *J Neural Transm* 2000, 60:S37-S58
- Senior K: New genes reveal major role for iron in neurodegeneration. *Lancet* 2001, 358:302
- Helfand SL: Neurobiology. Chaperones take flight. *Science* 2002, 295:809-810

38. Bonini NM: Chaperoning brain degeneration. *Proc Natl Acad Sci USA* 2002, 99(Suppl 4):16407–16411
39. Farah CA, Nguyen MD, Julien JP, Leclerc N: Altered levels and distribution of microtubule-associated proteins before disease onset in a mouse model of amyotrophic lateral sclerosis. *J Neurochem* 2003, 84:77–86
40. Liedtke W, Leman EE, Fyffe REW, Raine CS, Schubart UK: Stathmin-deficient mice develop an age dependent axonopathy of the central and peripheral nervous systems. *Am J Pathol* 2002, 160:469–480
41. Jin LW, Masliah E, Iimoto D, Deteresa R, Mallory M, Sundsmo M, Mori N, Sobel A, Saitoh T: Neurofibrillary tangle-associated alteration of Stathmin in Alzheimer's disease. *Neurobiol Aging* 1996, 17:331–341
42. Stieber A, Mourelatos Z, Gonatas NK: In Alzheimer's disease the Golgi apparatus of a population of neurons without neurofibrillary tangles is fragmented and atrophic. *Am J Pathol* 1996, 148:415–426
43. Cheon MS, Foundoulakis M, Cairns NJ: Decreased protein levels of Stathmin in adult brains with Down's syndrome and Alzheimer's disease. *J Neurol Transm* 2001, 61:S281–S286
44. Stieber A, Gonatas JO, Gonatas NK: Aggregates of ubiquitin and a mutant ALS-linked SOD1 protein correlate with disease progression and fragmentation of the Golgi apparatus. *J Neurol Sci* 2000, 173:53–62
45. Bruijn LI, Houseweart MK, Kato S, Anderson KL, Anderson SD, Ohama E, Reume AG, Scott RW, Cleveland DW: Aggregation and motor neuron toxicity of an ALS-linked SOD1 mutant independent from wild-type SOD1. *Science* 1998, 281:1851–1854
46. Brown JR RH: SOD1 aggregates in ALS: cause, correlate or consequence? *Nat Med* 1998, 4:1362–1364
47. Stieber A, Gonatas JO, Moore JS, Bantly A, Yim H-S, Yim MB, Gonatas NK: Disruption of the structure of the Golgi apparatus and the function of the secretory pathway by mutants G93A and G85R of Cu,Zn superoxide dismutase (SOD1) of familial amyotrophic lateral sclerosis. *J Neurol Sci* 2004, 219:45–53
48. Gosavi N, Lee H-J, Lee JS, Patel S, Lee S-J: Golgi fragmentation occurs in the cells with prefibrillar  $\alpha$ -synuclein aggregates and precedes the formation of fibrillar inclusion. *J Biol Chem* 2002, 277:48984–48992
49. Graves TK, Patel S, Dannies PS, Hinkle PM: Misfolded growth hormone causes fragmentation of the Golgi apparatus and disrupts endoplasmic reticulum-to-Golgi traffic. *J Cell Sci* 2001, 114:3685–3694
50. Yoshiyama Y, Zhang B, Bruce J, Trojanowski JQ, Lee M-Y V: Reduction of detyrosinated microtubules and Golgi fragmentation are linked to Tau-induced degeneration in astrocytes. *J Neurosci* 2003, 23:10662–10671
51. Stromer T, Ernsperger M, Gaestel M, Buchner J: Analysis of the interaction of small heat shock proteins with unfolding proteins. *J Biol Chem* 2003, 278:18015–18021
52. Pieri I, Cifuentes-Diaz C, Oudinet JP, Blondet B, Rieger F, Gonin S, Arrigo AP, Thomas Y: Modulation of HSP25 expression in the paralysed mouse mutant. *J Neurosci Res* 2001, 65:247–253
53. Dabir DV, Trojanowski JQ, Richter-Landsberg C, Lee VM-Y, Forman MS: Expression of the small heat-shock protein  $\alpha$ B crystallin in tauopathies and glial pathology. *Am J Pathol* 2004, 164:155–166
54. Takeuchi H, Niwa J-I, Hishikawa N, Ishigaki S, Tanaka F, Doyu M, Sobue G: Dofrin prevents cell death by reducing mitochondrial localizing mutant superoxide dismutase 1 in a neuronal cell model of familial amyotrophic lateral sclerosis. *J Neurochem* 2004, 89:64–72
55. Krapfenbauer K, Engidawork E, Cairns N, Foundoulakis M, Lubec G: Aberrant expression of peroxiredoxin subtypes in neurodegenerative disorders. *Brain Res* 2003, 967:152–160
56. Palacino JJ, Sagi D, Goldberg SM, Krauss S, Motz C, Wacker M, Klose JJ, Shen J: Mitochondrial dysfunction and oxidative damage in parkin-deficient mice. *J Biol Chem* 2004, 279:18614–18622
57. Valentine JS, Hart PJ: Misfolded CuZnSOD and amyotrophic lateral sclerosis. *Proc Natl Acad Sci USA* 2003, 100:3617–3622
58. Chen G, Gharib TG, Huang CC, Taylor JM, Misek DE, Kardias SL, Giordano TJ, Iannettoni MD, Orringer MB, Hanash SM, Beer DG: Discordant protein and mRNA expression in lung adenocarcinomas. *Mol Cell Proteomics* 2002, 1:304–313
59. Olsen M, Roberts SL, Ellenbrook BR: Disease mechanisms revealed by transcription profiling in SOD1–G93A transgenic mouse spinal cord. *Ann Neurol* 2001, 50:730–740
60. Yoshihara T, Ishigaki S, Yamamoto M, Liang Y, Niwa J-I, Takeuchi H, Doyu M, Sobue G: Differential expression of inflammation- and apoptosis-related genes in spinal cords of a mutant SOD1 transgenic mouse model of familial amyotrophic lateral sclerosis. *J Neurochem* 2002, 80:158–167
61. Kirby J, Menzies FM, Cookson MR, Busby K, Shaw PJ: Differential gene expression in a cell culture model of SOD1-related familial motor neuron disease. *Hum Mol Genet* 2002, 11:2061–2075
62. Allen S, Heath PR, Kirby J, Wharton SB, Cookson MR, Menzies FM, Banks RE, Shaw PJ: Analysis of the cytosolic proteome in a cell culture model of familial amyotrophic lateral sclerosis reveals alterations to the proteasome, antioxidant defenses and nitric oxide synthetic pathways. *J Biol Chem* 2003, 278:6371–6383
63. Malaspina A, Kaushik N, Belleruche DJ: Differential expression of 14 genes in amyotrophic lateral sclerosis spinal cord detected using gridded cDNA arrays. *J Neurochem* 2001, 77:132–145
64. Stieber A, Gonatas JO, Gonatas NK: Aggregates of mutant protein appear progressively in dendrites, in periaxonal processes of oligodendrocytes, and in neuronal and astrocytic perikarya of mice expressing the SOD1G93A mutation of familial amyotrophic lateral sclerosis. *J Neurol Sci* 2000, 177:114–123
65. Pramatarova A, Laganriere J, Roussel J, Brisebois K, Rouleau GA: Neuron-specific expression of mutant superoxide dismutase 1 in transgenic mice does not lead to motor impairment. *J Neurosci* 2001, 21:3369–3374
66. Lino MM, Schneider C, Caroni P: Accumulation of SOD1 mutants in postnatal motoneurons does not cause motoneuron pathology or motoneuron disease. *J Neurosci* 2002, 22:4825–4832
67. Gong YH, Parsadanian AS, Andreeva A, Snider WD, Elliott JL: Restricted expression of G86R superoxide dismutase in astrocytes results in astrocytosis but does not cause motoneuron degeneration. *J Neurosci* 2000, 20:660–665
68. Clement AM, Nguyen MD, Roberts EA, Garcia ML, Boillé S, Rule M, McMahon AP, Doucette W, Siwek D, Ferrante RJ, Brown Jr RH, Julien J-P, Goldstein LSB, Cleveland DW: Wild-type nonneuronal cells extend survival of SOD1 mutant motor neurons in ALS mice. *Science* 2003, 302:113–117